

FINAL REPORT 2016

For Public Release

Part 1 - Summary Details

Date Submitted:

Please use your TAB key to complete Parts 1 & 2. **CRDC Project Number:** CMSE1502 **Project Title:** The Contribution of Cellulose Crystallites to Fibre Strength **Project Commencement Date:** July 2014 **Project Completion Date:** June 2016 **CRDC Research Program:** 3 Customers Part 2 – Contact Details **Administrator:** Jo Cain - Administration Manager, Cotton Management & Improvement **Organisation: CSIRO Postal Address:** Locked Bag 59, 21888 Kamilaroi Hwy, Narrabri, NSW 2390 **Ph:** 02 6799 1513 E-mail: jo.cain@csiro.au Fax: Jeff Church **Principal Researcher: Organisation: CSIRO Postal Address:** 75 Pigdons Road, Waurn Ponds, VIC 3216 Ph: Fax: E-mail: **Supervisor:** Stuart Gordon – Principal Research Scientist **Organisation: Postal Address:** 75 Pigdons Road, Waurn Ponds, VIC 3216 **Ph:** 03 5246 4809 Fax: E-mail: stuart.gordon@csiro.au **Signature of Research Provider Representative:**

Revised June 2015 1 of 35

Part 3 – Final Report

(The points below are to be used as a guideline when completing your final report.)

Background

1. Outline the background to the project.

The objective of this project was to further investigate the relationship between cotton cellulose's crystalline structure and the fibre's tensile properties, as affected by chemical, genetic and/or environmental effects. In the end, because of time constraints, the variation in tensile properties as a result of these effects was not explored. Instead a select, well described group of fibre samples, controlled for micronaire, but with a wide range of tensile properties, in particular elongation, was selected for examination.

Whilst the application of IR spectroscopy and X-ray diffraction (XRD) to analyse the structure of cellulose is not new, this study utilised techniques not previously applied in the examination of cotton's crystallite structure. These included the application of the Australian Synchrotron small and wide angle (SAX/WAX) beamline to aligned arrays of single mature and immature fibres and the use of a confocal micro-Raman microscope with a polarizing lens to identify and measure different areas within single fibres. More routine measurements of fibre bundles using Fourier Transform Infrared Attenuated Transmission Reflectance (FTIR-ATR) and Raman spectroscopy were also made.

The first structural model for cellulose was proposed nearly 100 years ago and while the models have advanced since that time with the advent of new analytical technologies, they still do not wholly relate the contribution of cotton cellulose's structure, e.g., crystallinity index (CI), fibril size and orientation, to a fibre's tensile properties. There are a range of reasons for this gap in information. It is generally understood the CI, however it is measured, correlates well with cotton fibre strength, although only if the relationship is examined across the extreme range from an immature, developing fibre through to a fully mature fibre, or between fibres from different species [1-3]. Measuring structural differences between mature commercial Upland fibres is more difficult [4, 5]. One reason for this inability is that current methods used to analyse cotton cellulose's structure, e.g., XRD or infrared spectroscopy, have not been able to readily measure the structural properties of single, mature, unadulterated fibres because the incident beam has been too big or, if small enough, without enough flux to return a resolvable pattern or spectra. There is also the constraint of time to properly survey the variation in structure within a fibre at this scale.

Moreover, the application of infrared, Raman or X-ray beams to multiple fibre in bundles compromises the sensitivity of the measurement, because the measurement; (i) is now averaged across individual fibres of different structure and properties, (ii) includes fibres that are unaligned to the beam and (iii) in many studies, is of fibres that have been reduced to their smallest component unit, e.g., micro-fibrils, by milling the specimen before analysis. In each case, information regarding the structure of the fibre specimen is diluted or destroyed.

The interpretation of measured diffraction patterns or spectra is also not subject to a standardized technique and there are thus many interpretations taken with the data collected. For example, Terinte *et al* [6] reviewed five different approaches for integrating XRD patterns to calculate the crystallinity of cotton linters, microcrystalline (MC) cellulose from cotton linters after milling and a commercial MC powder. They concluded there was room for improvement concerning the particular X-ray method (reflection or transmission) used and then of the integration method used on the diffraction peaks to determine the CI.

A key ambition of this project was to bring new information about cotton's cellulose structure, via the application of new analytical methods to single fibres, to the relationship between cotton's cellulose structure and its tensile/mechanical properties. In the examination we considered cotton fibre's cellulose crystallites as long thin bundles of chain-molecules, similar in form to fibres in a yarn or sliver assembly. As per the interpretation by Astbury [7],

"the textile yarn or sliver is to the fibre as the fibre is to the chain-molecule", except that in reality the chains or crystallites are not discrete like a fibre but continuously bound through the cellulose complex.

The fibre-yarn analogy by Astbury [7] gives us a form to interpret many of the cellulose polymer's properties. For example, yarn tenacity is a function of yarn twist (fibril orientation), fibre fineness and length (fibril dimensions) and yarn evenness and the number of thin places in the yarn (fibril defects). These factors can be applied to interpret the cellulose complex for its mechanical (tensile) properties and to determine the chemical structural factors that ought to be measured and how.

The accepted crystal structure of native cellulose has changed little since that proposed by Meyer and Misch (1937) [8] and later modified by Frey-Wyssling. The unit cell, the cellobiose unit, has the dimensions of a = 0.835 nm, b = 1.030 nm and c = 0.79 nm, although there is variation around these depending on the cellulose and its form. Figure 1 illustrates the cell dimensions of cellulose I (native cellulose) as defined by Meyer and Misch (1937) [8]. Figure 2 illustrates the arrangement of cellobiose units within an elementary fibril as defined by Frey-Wyssling and Mülethaler (1963) [9] and the direction of the key crystalline lattices defined in terms of Miller index notation. Figures 3 through 7 from Evans $et\ al\ [10]$ illustrate the scale and architecture of cotton cellulose's structural dimensions, which are measured principally using XRD analysis.

In the crystalline regions of the cotton fibre, cellobiose units are covalently bound to form molecular chains that lie parallel in three-dimensional arrangements of high geometrical but variable order. In the 'amorphous' regions of the fibre, the molecular chains are arranged in less ordered states. It is important to recognize there are no sharp, measurable boundaries between the two regions. The chains of cellulose molecules associate with each other by forming hydrogen bonds. These join together to form microfibrils called crystallites. The microfibrils organize into macrofibrils, and the macrofibrils organize to form a fibre (see Figure 7). Thus cotton cellulose is not a single crystal but rather a crystalline aggregate of variable order. New information about its crystalline form as a mature fibre and the variation in this form are key if the cotton industry is to transform fibre properties, particularly tensile properties, beyond their current state.

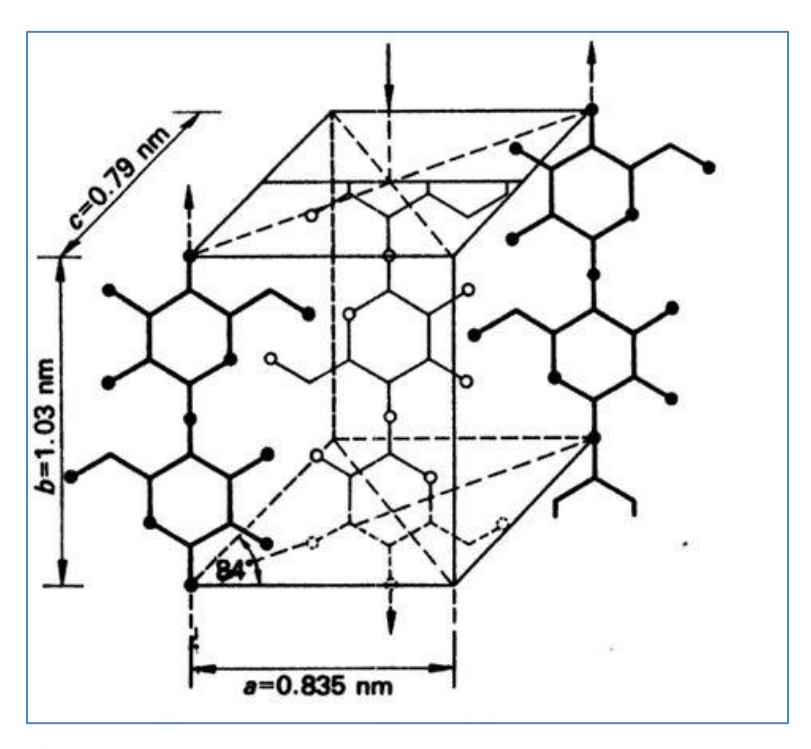


Figure 1 – Meyer and Misch's cellobiose unit and dimensions (1937).

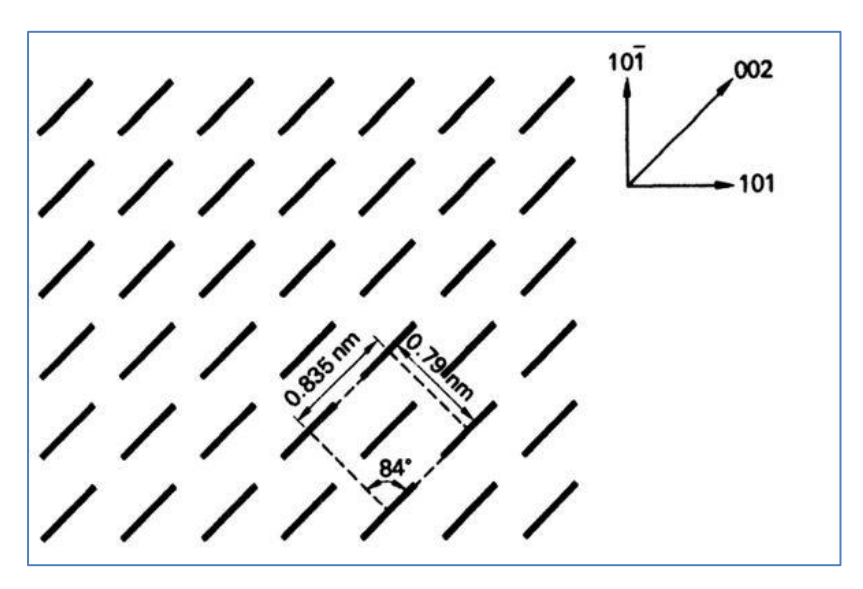


Figure 2 – Arrangement of cellulose chains in a transverse section of an elementary microfibril. Heavy lines represent glucose rings. Chains extend in and out of the page (Frey-Wyssling and Mülethaler, 1963).

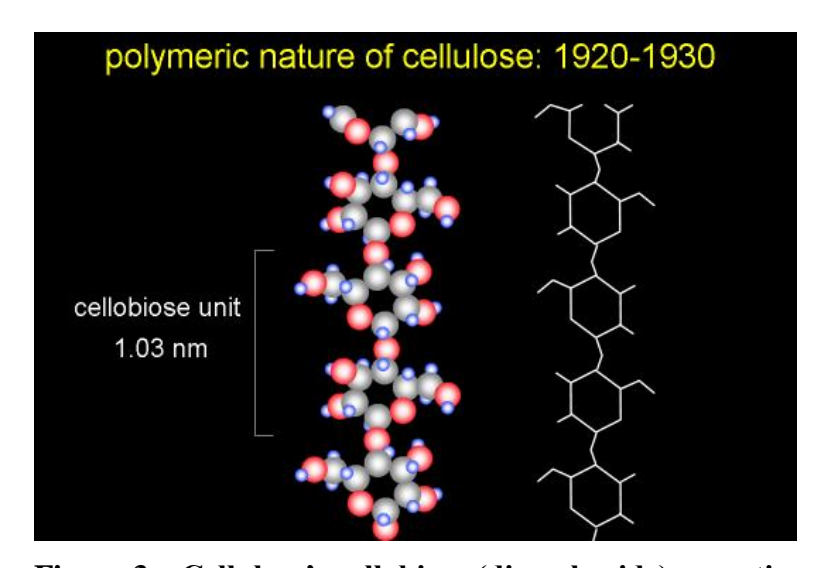


Figure 3 – Cellulose's cellobiose (disaccharide) repeating unit (C₆H₁₁O₅)_n.

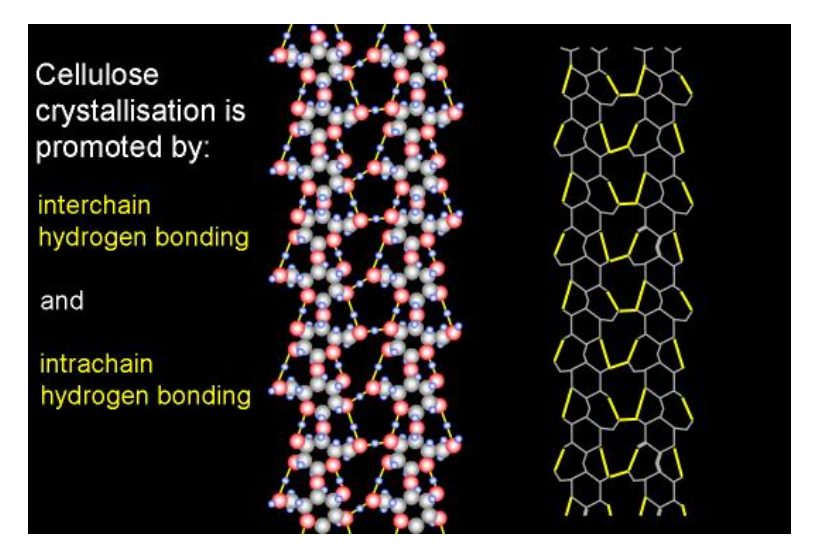


Figure 4 – Inter and intra hydrogen chain bonding between cellobiose units.

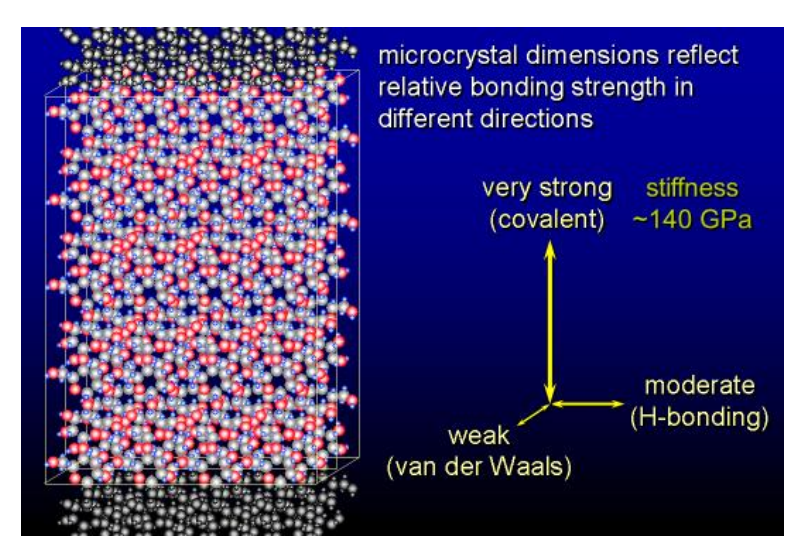


Figure 5 – Relative bonding strength of and between cellulose chains (fibrils) in different directions.

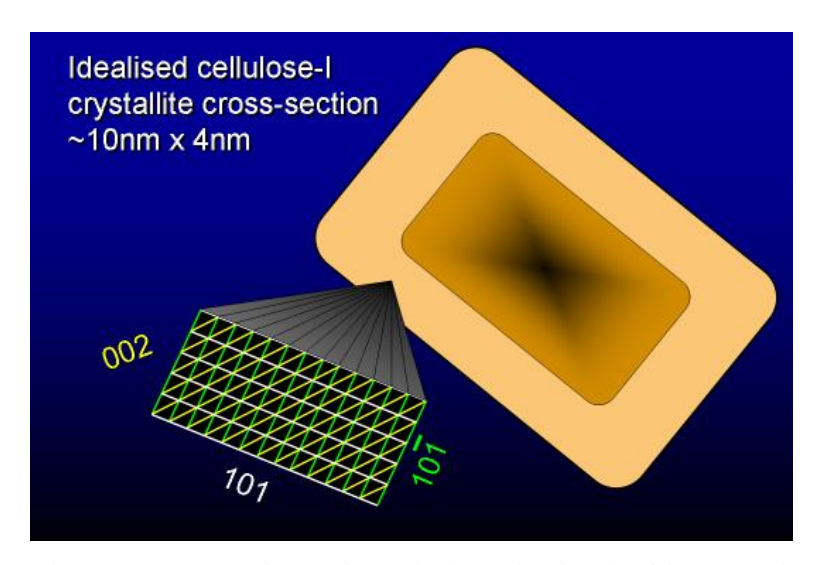


Figure 6 – The dimensions (Miller indices) of interest in the cellulose crystallite section and their arrangement within a fibril.

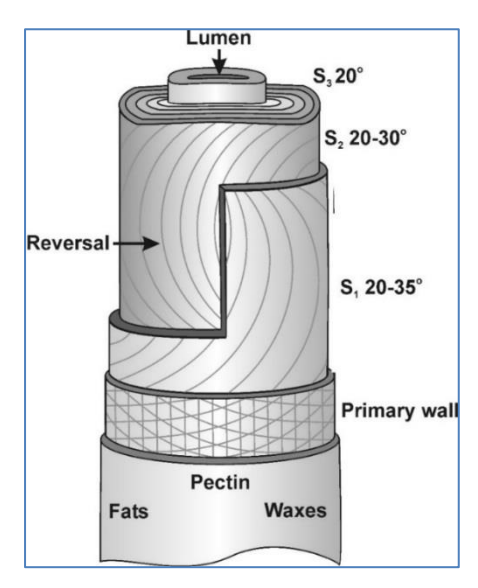


Figure 7 – The arrangement of micro and macro-fibrils and structural layers in mature cotton fibre.

Objectives

2. List the project objectives and the extent to which these have been achieved, with reference to the Milestones and Performance indicators.

ID	Milestone Title	Progress
1	Survey a range of cultivars	Achieved.
	for differences in x-ray,	A range of cotton fibre samples were selected and
	spectral and tensile	investigated by XRD, Fourier Transform Infrared
	measurements and select a	(FTIR) spectroscopy in attenuated total reflectance
	sub-set of samples for	(ATR) mode, confocal micro-Raman spectroscopy and
	further investigation.	a wide range of fibre metrology instruments. Selected
		samples were paired on the basis of their micronaire
		and elongation values. Immature and mature fibres
		from these samples were then separated for further
		examination by XRD and micro-Raman analysis.

2	Subject samples to a range of	Initiated but not pursued.
	chemical treatments to reveal	The above fibre samples were also subject to a range
	or remove structural 'layers'	of acid and alkali treatments. However, these
	or components of their	treatments were sporadic in their effect on fibre
	cellulose arrangement.	properties and generally did not significantly affect the
		crystalline nature of the fibre. Although, acid
		treatments affected fibre strength via hydrolysis of the
		cotton cellulose by the acid.

3	Publish additional details on	In progress.
	cotton cellulose structure	A paper detailing the experiments and results from this
	revealed by this project.	work for a journal such as Cellulose is currently being
		drafted.

Methods

3. Detail the methodology and justify the methodology used. Include any discoveries in methods that may benefit other related research.

Materials - samples

The physical and structural properties of cotton fibre, e.g., fibre maturity, elongation, are highly variable within a single cultivar as a result of environmental, genetic and G x E effects. Given the large number of tests to control these effects and the time required to test them, it was decided to limit the range of samples rather than trying to control these factors.

Table 1 below lists the seven samples selected for examination and their respective micronaire and elongation fibres values. The hypothesis for measuring cotton of similar micronaire but widely different elongation values was that analyses should also show large differences in cellulose structure for cotton that, are nominally the same in the market place.

It is acknowledged that other fibre properties influence or vary concurrently with fibre elongation bundle measurements, e.g., length, tenacity and maturity. However, controlling for all fibre properties is very difficult. To this consideration, pairs of the samples had at least one other property outside the micronaire and elongation values that was the same, or very different. Test values are coloured coded according to their paired micronaire sets.

Table 1 – Sample set: Micronaire x elongation (both as measured by HVI).

Micronaire	Elon. % (ID)	Elon. % (ID)
3.6	4.8 (3144)	6.8 (3117)
4.0	4.3 (3097)	7.6 (3119)
4.1	4.7 (3054)	
4.5	3.8 (3042)	6.7 (3159)

Analytical methods

Fibre samples were subject to a range of physical and chemical structure measurements. As part of the investigation new techniques were assessed for their ability to differentiate cotton fibres on the basis of their cellulose structure and if successful applied to the sample set. New techniques included application of the Australian Synchrotron SAX/WAX beamline and confocal-Raman microscopy. These required significant adaptation to enable very small (single), aligned fibre specimens, and even areas within single fibres, to be measured. Of these the XRD analyses provided the most detailed structural data. It is this data upon which conclusions in this project are primarily drawn.

Measurements by FTIR-ATR and FT-Raman spectroscopy were also made on fibre bundles. These are more standard analytical techniques that are applied successfully on a wide range of other materials but which have not really been able to delineate the structural characteristics of cotton samples of similar maturity and genetics. For example, Liu *et al* [11] matched fibre tenacity and elongation results to CI values calculated from FTIR-ATR spectra for a small set of commercial Upland and Pima varieties. There were poor relationships between CI values and tensile properties for the Upland cottons, although there was an increase in fibre tenacity with CI and fibre maturity for the Pima fibres. One of their main conclusions was that the tenacity/elongation values could be affected by multiple factors, such as crystallite size, which could not be measured by FTIR-ATR.

Descriptions of the methods used in this study appear below.

X-ray diffraction

X-ray diffraction in transmission mode using the Australian Synchrotron's small and wide angle X-ray (SAX/WAX) beamline on areas of the mature and immature fibres mounted in air. Individual fibres were selected from each sample and identified for their maturity using a polarized light microscope. Under this microscope fibres were viewed between the crossed polars and selected on the basis of their interference colour as per the method by ASTM D1442 [12] and used in the Cottonscope instrument. Five fibres of nominally the same maturity were mounted on purpose-built slotted slides that were positioned on a frame (Figure 8), which could be attached and positioned across the beamline (Figure 9). Figure 10 shows the scale of the SAX/WAX beamline at the AS.

The aligned fibre bundles were measured in five to six places along their length using a camera to locate regions of the aligned bundle that were close together (no air gap) and similar in terms of reflected light (an indicator of fibre fullness). The beam examining the fibre bundles was slitted to dimensions of $50 \times 350 \, \mu m$ with the bundle axis oriented along the longer length of the beamline. This meant the beam area was fully utilised by the fibres (minimal gaps), i.e., five fibres x $14 \, \mu m$ (average fibre width) = $70 \, \mu m$, thus encapsulating the entire beam for a length of $350 \, \mu m$. Technical specifications of the SAX/WAX beam and detector can be found in Appendix A1.

Two access periods were provided by the AS after applications in early 2014 (for access in October 2014) and early 2015 (for access in November 2015). The scope and methods

proposed in each investigation are detailed in the AS applications found in Appendices A2 (M8414) and A3 (M10068).



Figure 8 – Mounting frame for SAXS/WAX beamline being loaded with slides containing an array of aligned single fibres side-by-side.



Figure 9 – Mounting frame in position in front of WAX detector. A stepper motor and camera is used to guide frame into position of the beam. Orange tube in top LH corner contains X-ray crystal standard.



Figure 10 – Scale of the AS SAXS/WAX beamline and hutch. Dr Jeff Church examining the specimen frame position before measurement.

X-ray diffraction pattern analysis

Two methods were used to calculate CI from collected XRD diffraction patterns (see example patterns in Figure 11) of the single fibre arrays. Crystallinity index was expressed as (i) the sum of the de-convolved peaks over the total integrated area of the pattern and (ii) as the sum of the diffraction peaks over the sum of the peaks plus the amorphous fitted component. Both gave similar results (see Figure 12). The relevant CI ratios were then calculated as per Equation (1).

$$CI = \frac{A_c}{A_c + A_a} \tag{1}$$

where CI is the crystallinity index, A_c is the area of the crystallite peaks and A_a is the area of the amorphous peaks.

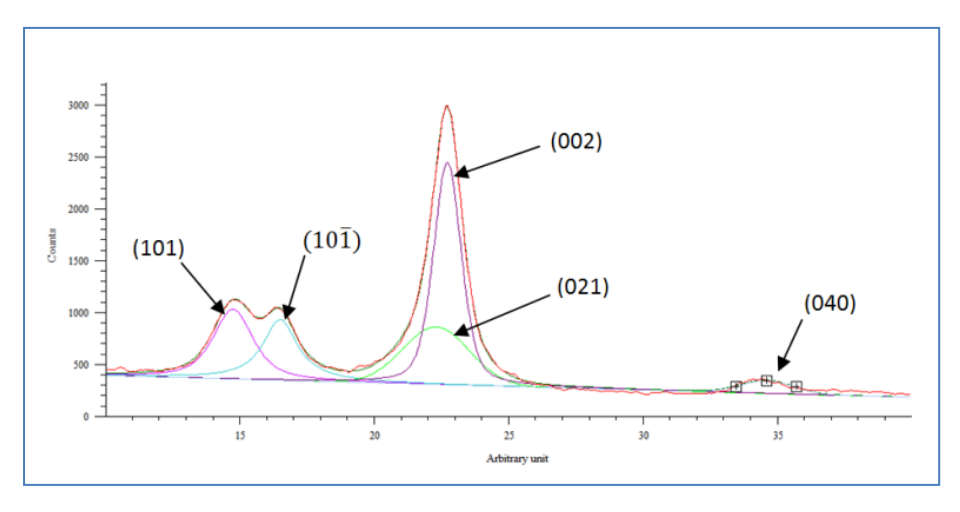


Figure 11 – Typical diffraction pattern for crystalline cellulose I (cotton) showing position (and intensity) of crystallite orientations (101, 1-01, 002, 021 and 040) and integration of peaks across the 2θ range 10° to 40° (x-axis).

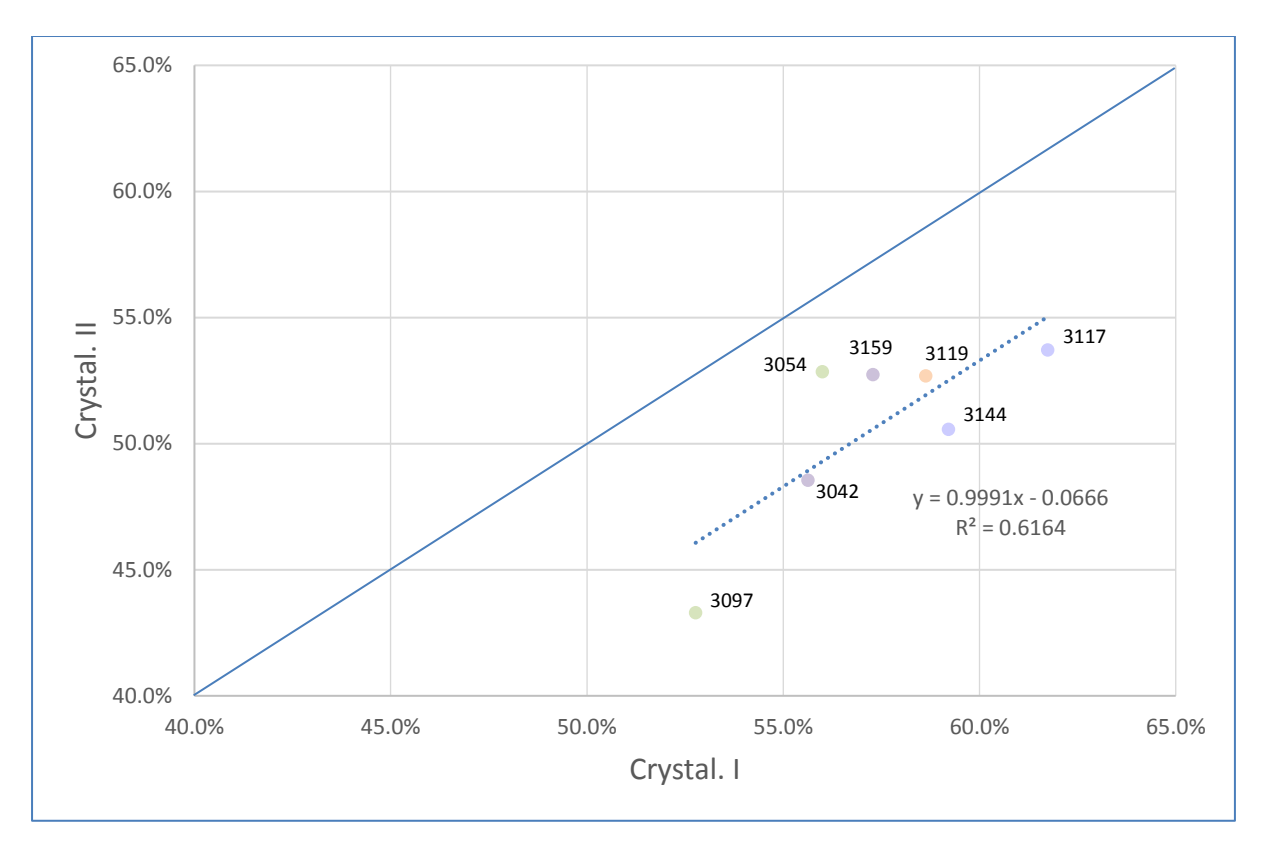


Figure 12 – Relationship between average crystallinity index measurements by two similar methods for the sample set.

Dimensions of the Miller indices were calculated using the Scherrer Equation [13] – see Equation 2.

$$\tau = \frac{\kappa\lambda}{\beta\cos\theta} \tag{2}$$

where τ is the mean size of the ordered (crystalline) domains, which may be smaller or equal to the grain size; K is a dimensionless shape factor, with a value typically of about 0.9 although this varies with the actual shape of the crystallite. A value of 0.9 was used in calculations in this work. λ is the X-ray wavelength (in this case 0.15404 nm); β is the line broadening (in radians) at half the maximum intensity (at full width half maximum (FWHM)) after subtracting the instrumental line broadening and θ is the Bragg angle (in degrees).

Cellobiose crystallite dimensions (a, b and c) and density were calculated using the formulae by Foreman and Jakes [14].

Fourier Transform infrared spectroscopy using Attenuated Total Reflectance

Fourier Transform Infrared (FTIR) spectroscopy using an Attenuated Total Reflectance (ATR) accessory fitted to a Perkin Elmer Spectrum 100 Fourier Transform infrared spectrometer. Small fibre bundles were aligned by hand and placed across the diamond ATR crystal (2 mm diameter) so there were multiple fibres laid across the crystal face. Recorded spectra are 16 co-added scans replicated in six places with the specimen held at a set holding pressure (70 mN).

All spectra were linear baseline corrected and normalised prior to analysis using principal components analysis (PCA) and partial least squares (PLS) to summarize the measured variance and responses from the cotton samples.

Fourier Transform Raman spectroscopy

FT-Raman analysis was conducted using a Bruker RFS 100 spectrometer (1064 nm). Small bundles of fibre samples were compressed, randomly orientated, into the instrument's

compression cell. Spectra were collected using 750 mW power and 512 co-added scans. Six replicates were tested per sample.

Similarly to the FTIR-ATR analysis, spectra were subjected to baseline correction and normalisation and then analysed using PCA and PLS to summarize the measured variance and responses from the cotton samples.

Confocal micro-Raman microscopy

Confocal micro-Raman spectroscopy was carried out using a Renishaw inVia confocal micro-Raman microscope fitted with polarizing lenses that were used to identify specific 'mature' and 'immature' areas on single aligned cotton fibres. Single fibres were mounted on a glass microscope slide using double sided adhesive tape. Two types of analysis were attempted with this instrument:

- Raman spectra were obtained using the polarizing lens to identify specific areas on Sample 3054. A 785 nm laser with a pin hole aperture, to produce a circular beam (of 0.8 µm), was used at, 50% laser power (estimated 7.3 mW) through the x100 objective. Each spectrum was a result of a 10 s exposure and five co-added scans.
- A 514 nm laser beam (area $\approx 1~\mu m$) at 100% laser power (estimated 8 mW) was used to investigate spectral differences through the cotton fibre using the x100 objective. The sample was exposed to the beam for 15 s and a total of 20 scans co-added (to decrease noise) at each incremental step into the fibre. Spectra were collected from 15 steps (at 1 μm intervals) through a mature fibre specimen from Sample 3054 only.

Physical fibre testing

The physical properties of the samples were measured using HVI, AFIS and Favimat according to standard test methods. Cottonscope measurements were made according to the CSIRO standard test method while cross-section property measurements were made according to the embedding and cross-sectional analysis methods by Boyleston *et al* [15] and Hequet *et al* [16].

Chemical preparation/modification of fibre samples

Fibre samples subject to scouring, hydrolysis and swelling treatments were subject to preliminary examinations by FTIR-ATR and FT-Raman spectroscopy. However, inconsistency in the chemical treatment between and within fibres (along their length), the limited scale of change in the fibre's structural properties and limitations on time meant further investigation of these samples was not pursued.

Regulte

4. Detail and discuss the results for each objective including the statistical analysis of results

Tables 2, 3, 4, 5, 6 and 7 list the measured values from various instrument analyses; XRD, cross-sectional analysis (+ Cottonscope maturity ratio), HVI and Favimat (+ Cottonscope linear density) respectively. There were significant correlations between physical test values within the set based on known relationships, e.g., correlations between cross-section properties measured by cross-section analysis, AFIS, Cottonscope and HVI. And similarly between length and tensile measurements. However, the extent of these relationships was not explored in this study.

The focus of the analysis here was to measure the best correlations between the above physical properties and structural properties, particularly those from XRD measurements at the Australian Synchrotron. Spectral data from FTIR-ATR and FT-Raman were not assessed against physical fibre data because component analysis did not reveal distinct difference between samples (see later in discussion). This reflected recent work, e.g., the work by Liu *et*

al [12], which did not show differences in CI between commercial Upland cottons of similar maturity.

Table 2 – XRD crystallinity, lattice dimensions and crystallite size for immature and mature fibre specimens. Sample ID followed by I represents immature and M represents mature specimens respectively.

		Crystal. I	101	1-01	021	002	040	a (nm)	b (nm)	c (nm)	V (nm³)	ρ (kg/m³)
3097 I Av	verage	53%	3.77	5.89	11.47	7.71	5.46	0.821	1.046	0.795	0.672	1603
St	tdev	1%	0.09	0.08	0.07	0.07	0.06	0.001	0.001	0.000	0.001	2
3097 M A	verage	53%	3.75	6.08	11.63	7.80	5.48	0.818	1.046	0.794	0.669	1608
St	tdev	3%	0.07	0.04	0.09	0.08	0.13	0.001	0.001	0.000	0.001	2
3119 I A	verage	56%	4.13	5.12	10.81	7.72	6.13	0.824	1.039	0.794	0.670	1607
St	tdev	2%	0.20	0.96	0.45	0.18	1.09	0.001	0.002	0.000	0.002	5
3119 M A	verage	61%	4.50	5.87	10.76	7.29	7.28	0.821	1.040	0.794	0.667	1613
St	tdev	3%	0.03	0.08	0.15	0.02	1.79	0.001	0.002	0.000	0.001	2
3144 I A	verage	59%	4.50	5.77	11.04	7.44	5.85	0.820	1.043	0.794	0.669	1609
	tdev	1%	0.06	0.11	0.13	0.02	0.26	0.001	0.000	0.000	0.001	1
3144 M A	verage	60%	4.53	5.84	10.72	7.42	5.52	0.820	1.042	0.794	0.669	1609
St	tdev	2%	0.08	0.13	0.15	0.04	0.15	0.000	0.001	0.000	0.001	1
3159 I A	verage	57%	4.17	6.02	11.68	7.69	6.74	0.823	1.041	0.794	0.671	1605
St	tdev	2%	0.03	0.07	0.20	0.04	0.80	0.001	0.001	0.000	0.001	3
3159 M A	verage	57%	4.55	5.91	11.47	7.69	6.43	0.823	1.044	0.795	0.673	1600
St	tdev	2%	0.05	0.12	0.05	0.04	1.11	0.001	0.002	0.000	0.000	1
3054 I A	verage	52%	4.27	5.43	10.57	7.25	5.97	0.819	1.041	0.794	0.667	1614
St	tdev	5%	0.14	0.21	0.30	0.16	0.48	0.002	0.001	0.000	0.001	3
3054 M A	verage	60%	4.65	6.13	11.29	7.72	5.65	0.820	1.043	0.793	0.668	1612
St	tdev	2%	0.12	0.19	0.18	0.09	0.02	0.001	0.002	0.000	0.001	2
3117 I A	•	63%	4.53	5.65	10.82	7.37	9.46	0.823	1.039	0.794	0.669	1608
	tdev	2%	0.08	0.01	0.11	0.02	2.52	0.000	0.001	0.000	0.000	1
3117 M A	verage	61%	4.44	5.73	10.55	7.18	5.99	0.821	1.041	0.794	0.670	1608
St	tdev	2%	0.07	0.08	0.10	0.07	0.84	0.000	0.001	0.000	0.001	1
3042 I A	•	56%	4.66	5.65	10.95	5.69	5.55	0.821	1.044	0.796	0.672	1603
	tdev	3%	0.08	0.13	0.40	0.03	0.13	0.001	0.000	0.002	0.002	5
3042 M A	•	55%	4.55	5.56	11.12	7.45	5.73	0.821	1.045	0.795	0.672	1601
St	tdev	1%	0.06	0.08	0.17	0.08	0.15	0.001	0.001	0.000	0.001	2

Table 3 – Average XRD crystallinity, Miller index and crystallite size.

Bale ID	Crystal. I	Crystal. II	101	1 <u>01</u>	021	002	040 b	eta (deg)	a (nm)	b (nm)	c (nm)	V (nm³) ρ	(kg/m³)
3042	56%	49%	4.60	5.60	11.04	6.57	5.64	80.27	0.821	1.044	0.795	0.672	1602
3054	56%	53%	4.46	5.78	10.93	7.49	5.81	80.28	0.819	1.042	0.793	0.667	1613
3097	53%	43%	3.76	5.99	11.55	7.76	5.47	80.06	0.819	1.046	0.794	0.670	1606
3117	62%	54%	4.49	5.69	10.68	7.27	7.73	80.20	0.822	1.040	0.794	0.669	1608
3119	59%	53%	4.32	5.50	10.78	7.50	6.71	80.17	0.823	1.040	0.794	0.669	1610
3144	59%	51%	4.51	5.81	10.88	7.43	5.68	80.30	0.820	1.043	0.794	0.669	1609
3159	57%	53%	4.36	5.96	11.57	7.69	6.58	80.21	0.823	1.043	0.794	0.672	1602

Table 4 – HVI test results (fibre bundle analysis (n = 10 test specimens/sample))

ID	Mic.	Len. inch	Uni. %	Ten. g/tex	Elon. %	Leaf	Rd	+ b
	HVI	HVI	HVI	HVI	HVI	HVI	HVI	HVI
3042	4.49	1.08	82.6	33.3	3.8	1.0	77.9	10.8
3054	4.10	1.04	81.9	28.6	4.7	1.0	77.2	11.8
3097	4.00	0.96	79.0	23.9	4.3	1.0	77.3	11.1
3117	3.58	0.99	81.3	25.2	6.8	1.0	79.0	11.9
3119	4.00	1.08	83.2	27.8	7.6	1.0	77.4	11.2
3144	3.58	1.08	80.4	28.7	4.8	1.0	77.9	12.1
3159	4.49	1.02	81.6	25.0	6.7	1.0	73.2	9.3

Table 5 – Favimat test results (single fibre analysis (n = 330 fibres/sample))

ID	H mtex	Elon. %	Fmax N	Work	Ten. g/tex	H dtex
	C'scope	F'mat	F'mat	F'mat	F'mat	F'mat
3042	162	4.77	5.33	0.165	31.52	1.70
3054	180	4.34	5.28	0.147	31.76	1.68
3097	198	4.32	5.04	0.15	30.85	1.65
3117	197	5.06	4.56	0.16	25.80	1.79
3119	182	6.28	4.76	0.194	26.42	1.81
3144	198	4.63	4.70	0.145	28.75	1.65
3159	218	5.82	5.21	0.211	25.10	2.10

Table 6 – Cross-sectional analysis and Cottonscope test results (single fibre analysis (XS analysis = >3000 fibres/sample; Cottonscope = >20,000 fibres/sample))

ID	XSA um ²	H mtex	CV%	Peri. um	CV%	Theta	CV%	MR
	XS	XS	XS	XS	XS	XS	XS	C'scope
3042	102.3	155.5	2.8	50.6	1.6	0.517	1.3	0.86
3054	96.1	146.1	1.9	49.8	1.3	0.505	1.6	0.86
3097	106.7	162.2	7.5	54.5	3.9	0.471	1.9	0.79
3117	105.8	160.8	3.3	57.5	2	0.425	4.2	0.72
3119	108.2	164.5	4	54.8	1.7	0.474	3.2	0.77
3144	91.6	139.2	2.6	49.8	1.4	0.483	2.6	0.83
3159	125.5	190.8	3.6	58.1	2.3	0.49	2.3	0.76

Table 7 – AFIS test results (single fibre analysis (n = >3000 fibres/sample))

ID	Nep cnt/g	SCN cnt/g	Lw inch	SFC _w %	UQL inch	MR	IFC %	H mtex
	AFIS	AFIS	AFIS	AFIS	AFIS	AFIS	AFIS	AFIS
3042	106	3	0.93	9.2	1.13	0.90	7.5	169
3054	172	9	0.89	10.1	1.07	0.87	8.5	161
3097	237	5	0.80	15.1	0.98	0.86	7.8	169
3117	455	24	0.81	16.0	1.00	0.78	11.6	158
3119	314	12	0.92	10.2	1.12	0.83	9.1	165
3144	470	32	0.90	13.0	1.12	0.83	10.0	153
3159	223	10	0.84	13.9	1.03	0.82	9.4	170

Differences in XRD values between samples based on fibre maturity (as per Table 2) were tested but the expected differences did not bare out as hypothesized, i.e., the hypothesis that immature fibres would have different structural dimensions to mature fibres. This was because selecting and identifying single immature fibres from the samples proved difficult. It is assumed that fibre maturity is normally distributed in a sample, albeit with a negative skew, such that there should be a clear population of immature fibres in each sample. However, the practice of physically selecting a single fibre, particularly one of a length that enables it to be laid and stretched commonly with other selected fibres across the width of the mounting slide is difficult and subject to a length bias. This bias, which favours long mature, unbroken fibres, is difficult to overcome in routine analysis. Assessment of maturity via interference colours as per [11] also proved challenging. There is a continuum of colours in the interference spectra and determining a cut-off point, when a fibre moves from immature to mature, is difficult without application of an objective colour image analysis system such as that used in Cottonscope.

Figures 12 to 14 show dimensions of the lattice (Miller) indices (101 and 1-01, 002 and 021 and 040) dimensions for mature and immature specimens from each sample. As per the challenges described there are no consistently significant or obvious differences between mature and immature fibre specimens in these tests. Given the ambiguity in selecting immature from mature fibre specimens, where it was likely that less mature but still mature fibres were selected as immature fibres, indices values were accepted as being equal and averaged for each sample (see Table 3). Apparent however are significant, albeit subtle differences between paired samples, i.e., samples of the same micronaire but different elongation.

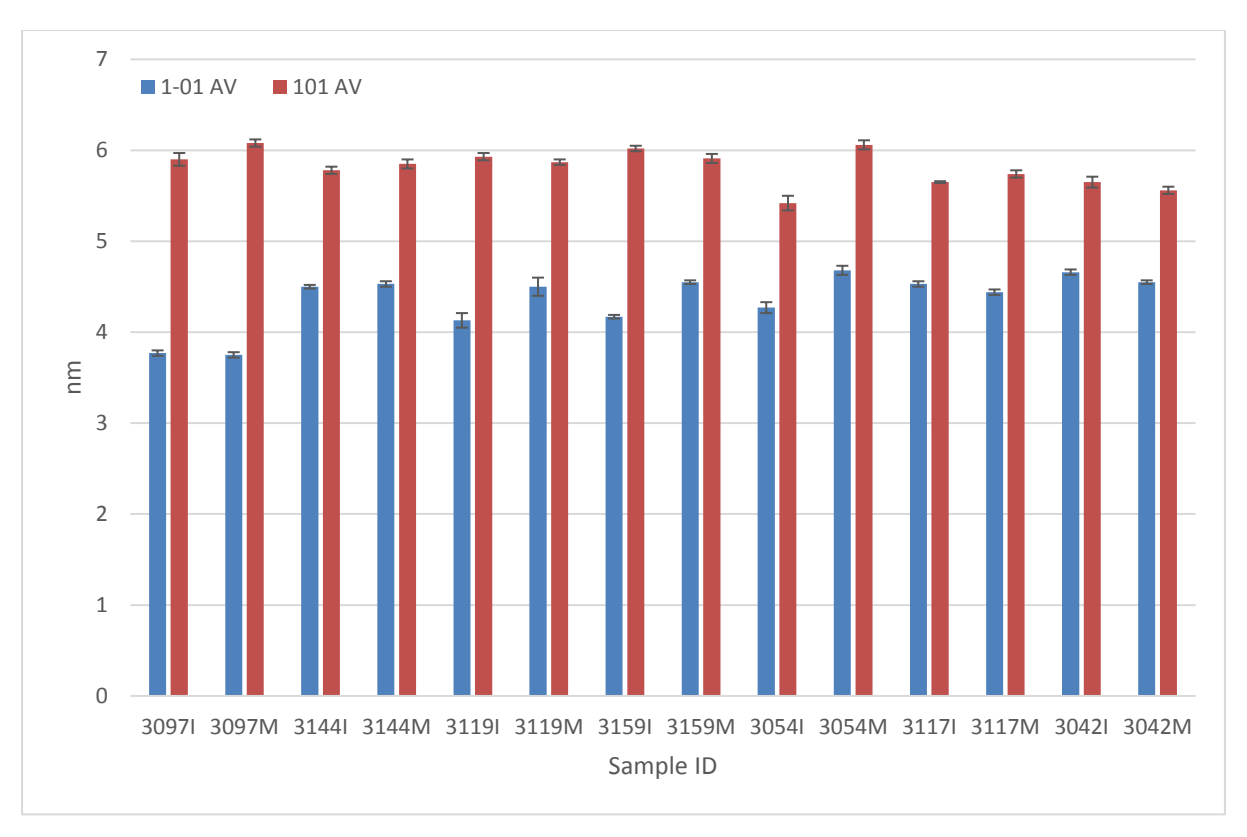


Figure 12 - XRD measured Miller indices 101 and 1-01 for mature and immature fibre arrays. Error bars represent standard error for average values (n = 5).

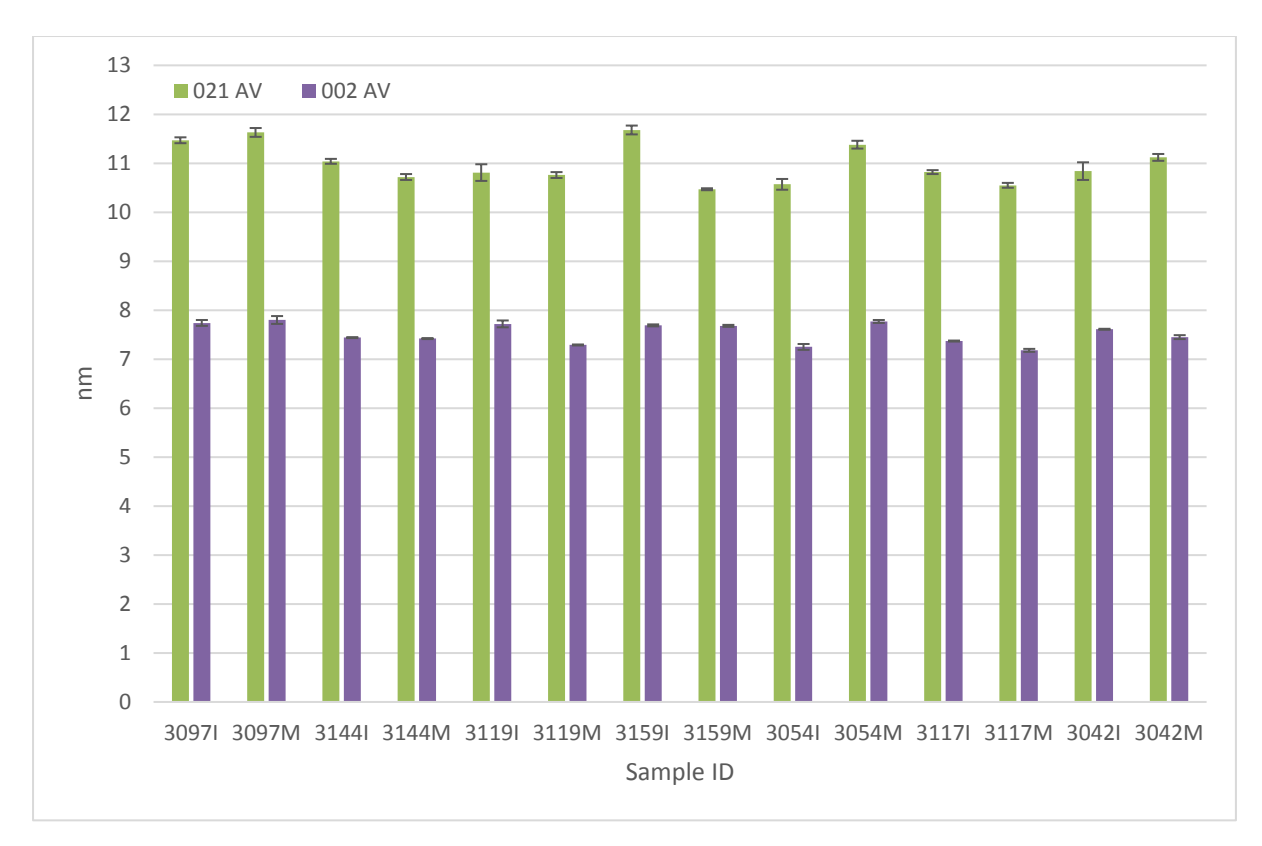


Figure 13 - XRD measured Miller indices 021 and 002 for mature and immature fibre arrays. Error bars represent standard error for average values (n = 5).

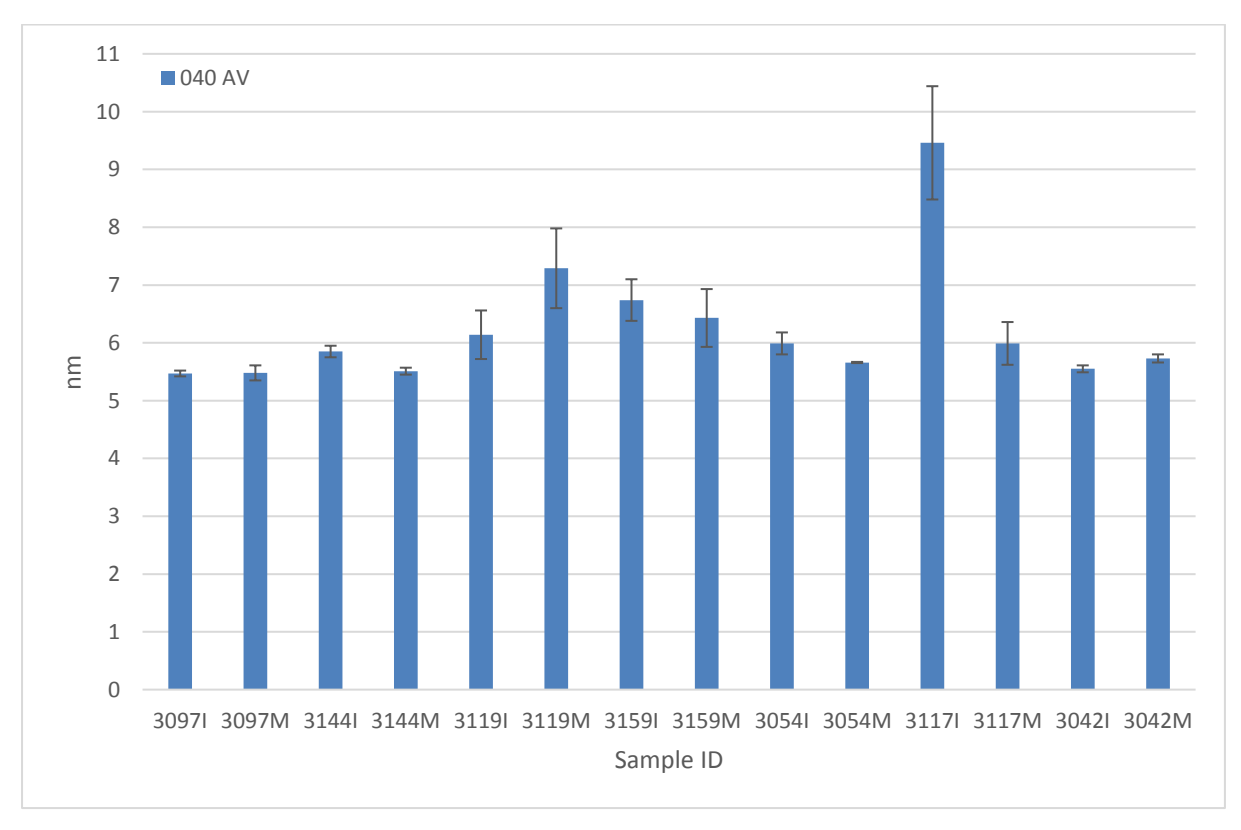


Figure 14 - XRD measured Miller index 040 for mature and immature fibre arrays. Error bars represent standard error for average values (n = 5).

Regression Analysis

Structural measurements by XRD were tested for their ability to predict (as independent variables (IV)) physical fibre properties such as tenacity and elongation as measured by HVI and Favimat, using a forward stepwise regression approach. Acknowledging the small size of the regression set, independent or predictor variables into these equations were tested by setting the alpha to enter (α_E) the equation at 0.1, rather than the default of 0.15, although entry at the 0.15 level was also tested. The number of predictor variables was also limited to a maximum of two. Stepwise regressions were performed using Minitab 17.

Table 8 lists the regression statistics (R², R²-adjusted and R²-predicted) for selected structural predictor variables for dependent variables theta by cross-sectional analysis, maturity ratio by Cottonscope and AFIS, micronaire, tenacity and elongation by HVI and tenacity and elongation by the Favimat.

Table 8 – Forward stepwise regressions. Cellulose structural elements selected as independent variables to predict cotton fibre cross-section and tensile properties.

Dependent var.	Independent 'structural' varia	ble(s) (IV) in order of selection
	$\alpha_{\rm E} = 0.1$	$\alpha_{\rm E}=0.15$
ΧS θ	IV = 040	IVs = 040 + Crystallinity II
	$R^2 = 56.6\%, p = 0.051$	$R^2 = 77.2\%, p = 0.023, 0.130$
	R^2 adj. = 47.9%	R^2 adj. = 65.8%
	R^2 pred. = 0.0%	R^2 pred. = 14.1%
MR Cottonscope	IVs = 040 + 101	IVs = 040 + 101
_	$R^2 = 92.5\%, p = 0.002, 0.025$	$R^2 = 92.5\%, p = 0.002, 0.025$
	R^2 adj. = 88.8%	R^2 adj. = 88.8%
	R^2 pred. = 86.3%	R^2 pred. = 86.3%
MR AFIS	IVs = 040 + 002	IVs = 040 + 002
	$R^2 = 85.4\%, p = 0.014, 0.093$	$R^2 = 85.4\%, p = 0.014, 0.093$
	R^2 adj. = 78.1%	R^2 adj. = 78.1%
	R^2 pred. = 33.7%	R^2 pred. = 33.7%
HVI Mic.	No terms selected	$IVs = V$ and ρ
		$R^2 = 98.2\%, p = 0.000$
		R^2 adj. = 97.3%
		R^2 pred. = 93.8%
HVI Ten.	IV = 002	IV = 002
	$R^2 = 71.2\%, p = 0.017$	$R^2 = 71.2\%, p = 0.017$
	R^2 adj. = 65.7%	R^2 adj. = 65.7%
	R^2 pred. = 54.6%	R^2 pred. = 54.6%
HVI Elong.	IV = 040	IV = 040
_	$R^2 = 70.2\%, p = 0.019$	$R^2 = 70.2\%, p = 0.019$
	R^2 adj. = 64.2%	R^2 adj. = 64.2%
	R^2 pred. = 0.0%	R^2 pred. = 0.0%
F'mat Ten.	IV = a	IVs = a + 002
	$R^2 = 75.7\%, p = 0.011$	$R^2 = 88.1\%, p = 0.007, 0.112$
	R^2 adj. = 70.9%	R^2 adj. = 82.1%
	R^2 pred. = 63.8%	R^2 pred. = 26.4%
F'mat Elong.	IV = a	IV = a
	$R^2 = 82.2\%, p = 0.005$	$R^2 = 82.2\%, p = 0.005$
	R^2 adj. = 78.6%	R^2 adj. = 78.6%
	R^2 pred. = 66.6%	R^2 pred. = 66.6%

The regressions show that variation in the dimensions of the 002 and 040 crystallite lattices (as per Figure 11) and the 'a' dimension of cellobiose unit corresponded closely with differences in fibre maturity and tensile properties. Additional terms entered at α_E of 0.15 did not improve the predictability of the generated equation. The exception to this were the IVs selected for micronaire when the α_E was opened to 0.15. No IVs were selected to predict micronaire when the α_E was set at 0.1.

Figures 15-19 show XY plots of maturity and tensile properties with the selected structural measurements. The best relationships in terms of statistical correlation and significance, and thus confidence in their causal relationship, were Cottonscope maturity with the 040 and 101 lattice dimensions and Favimat tenacity and elongation measurements with the 'a' dimensions of the cellobiose unit. Further analysis is required to establish the contribution of these elements to the mechanical properties of cotton fibre. HVI tenacity and elongation values suffered from the errors, e.g., inter-fibre friction and mass estimation, associated with bundle testing, although the HVI tenacity relationship with the 002 lattice dimensions was robust and deserves further attention.

Interestingly, micronaire values corresponded closely with the volume of the cellobiose unit, i.e., the cellobiose dimensions a, b and c, which are used to calculate volume (V) and density (ρ) of the unit cell. It is noted that the selected IVs for micronaire, cellobiose unit volume and density, are essentially reciprocals of each other (see Figures 20 and 21).

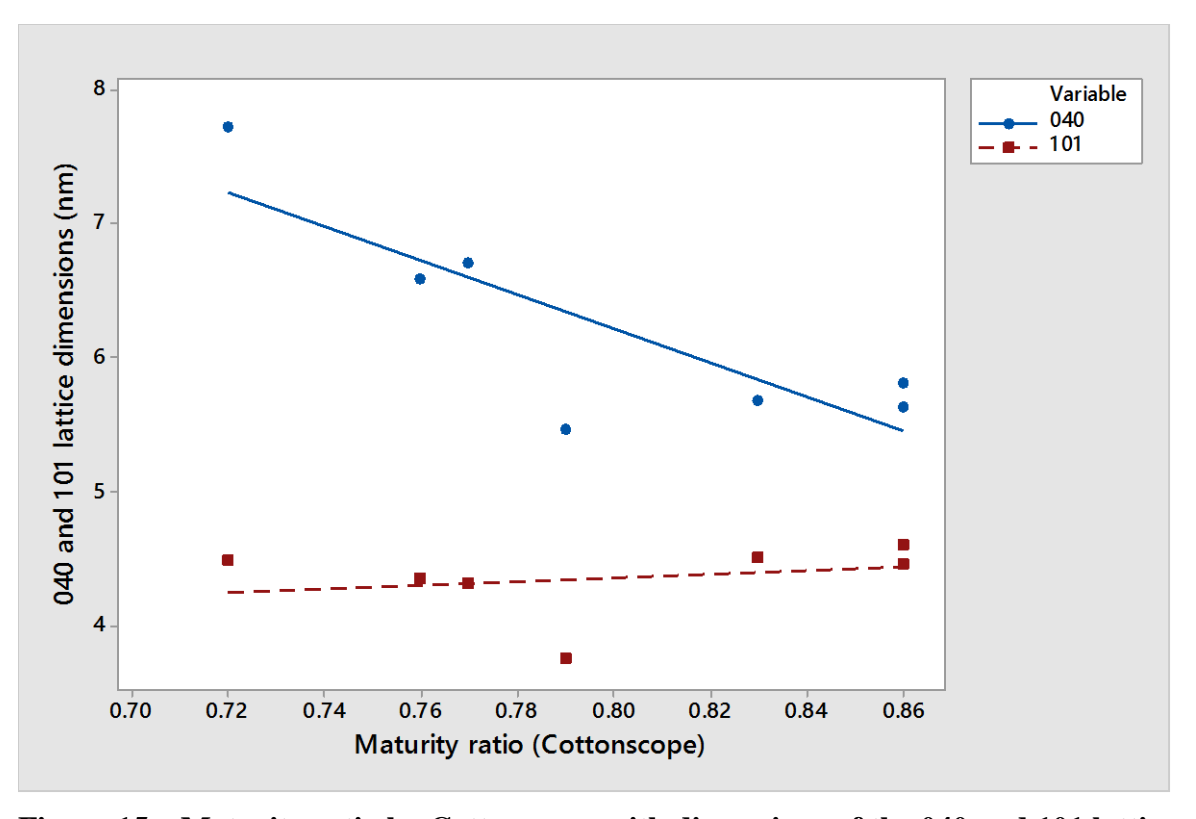


Figure 15 – Maturity ratio by Cottonscope with dimensions of the 040 and 101 lattices in cellulose.

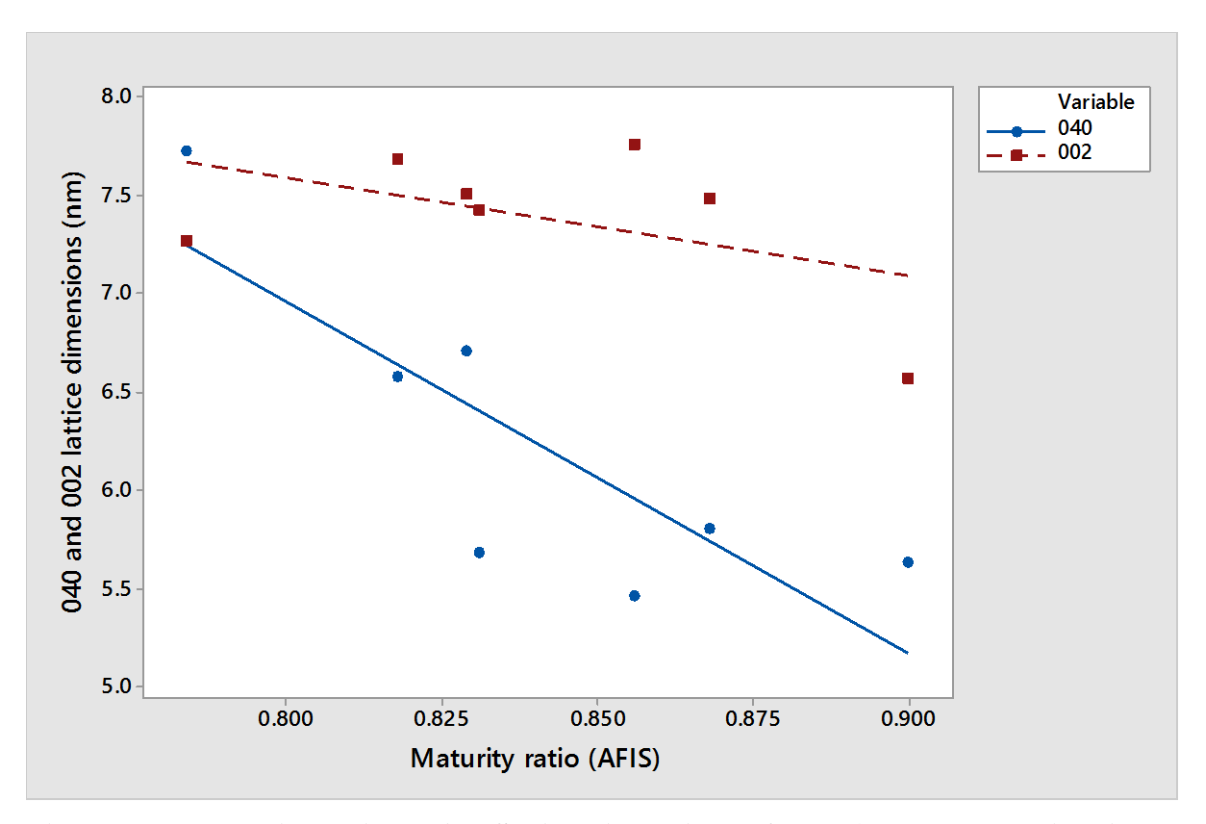


Figure 16 – Maturity ratio by AFIS with dimensions of the 040 and 002 lattices in cellulose.

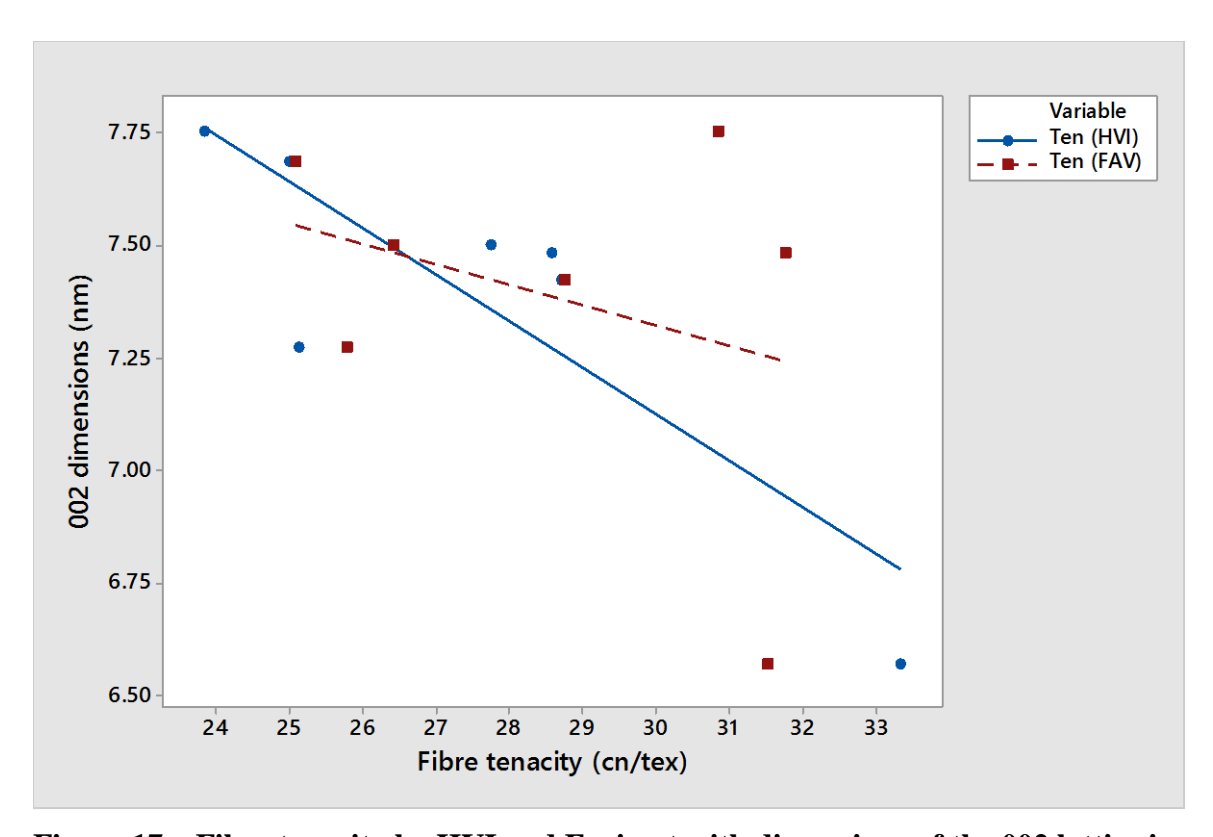


Figure 17 – Fibre tenacity by HVI and Favimat with dimensions of the 002 lattice in cellulose.

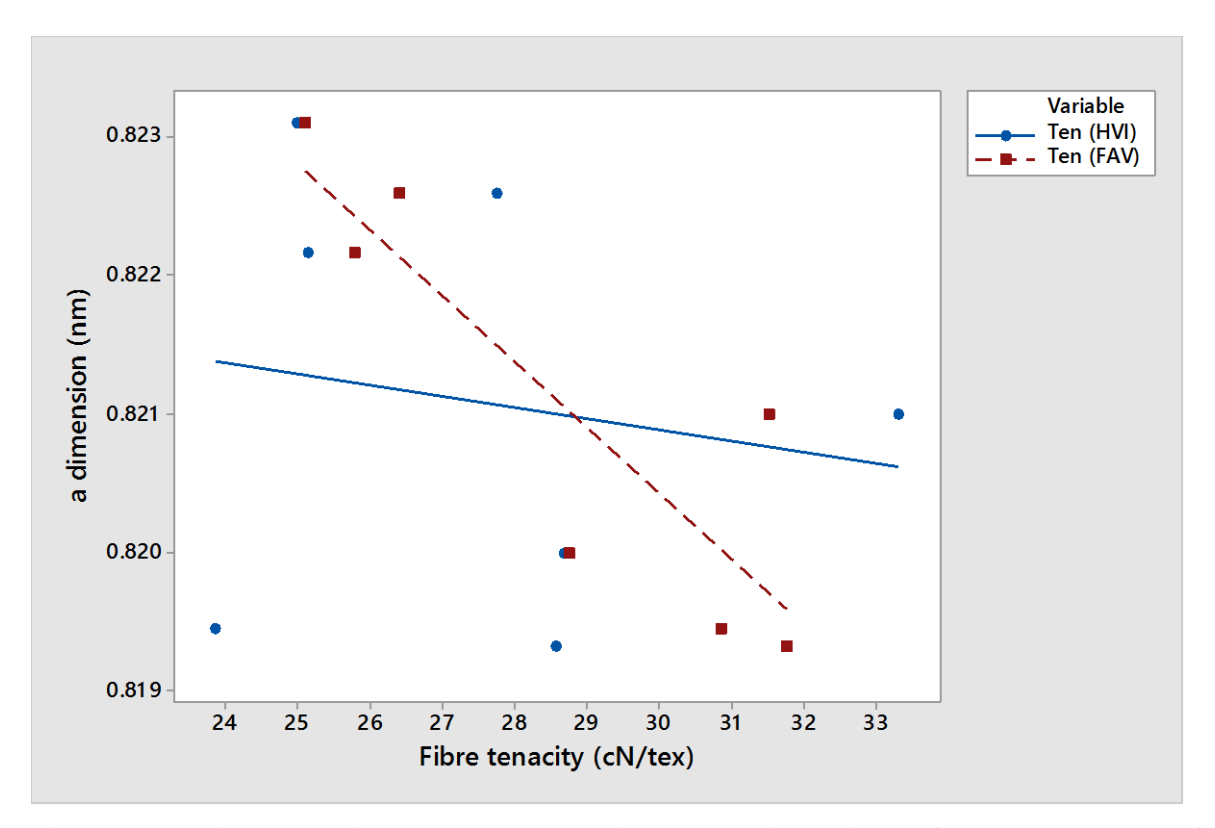


Figure 18 – Fibre tenacity by HVI and Favimat with dimensions of the 'a' direction of the cellobiose unit in cellulose.

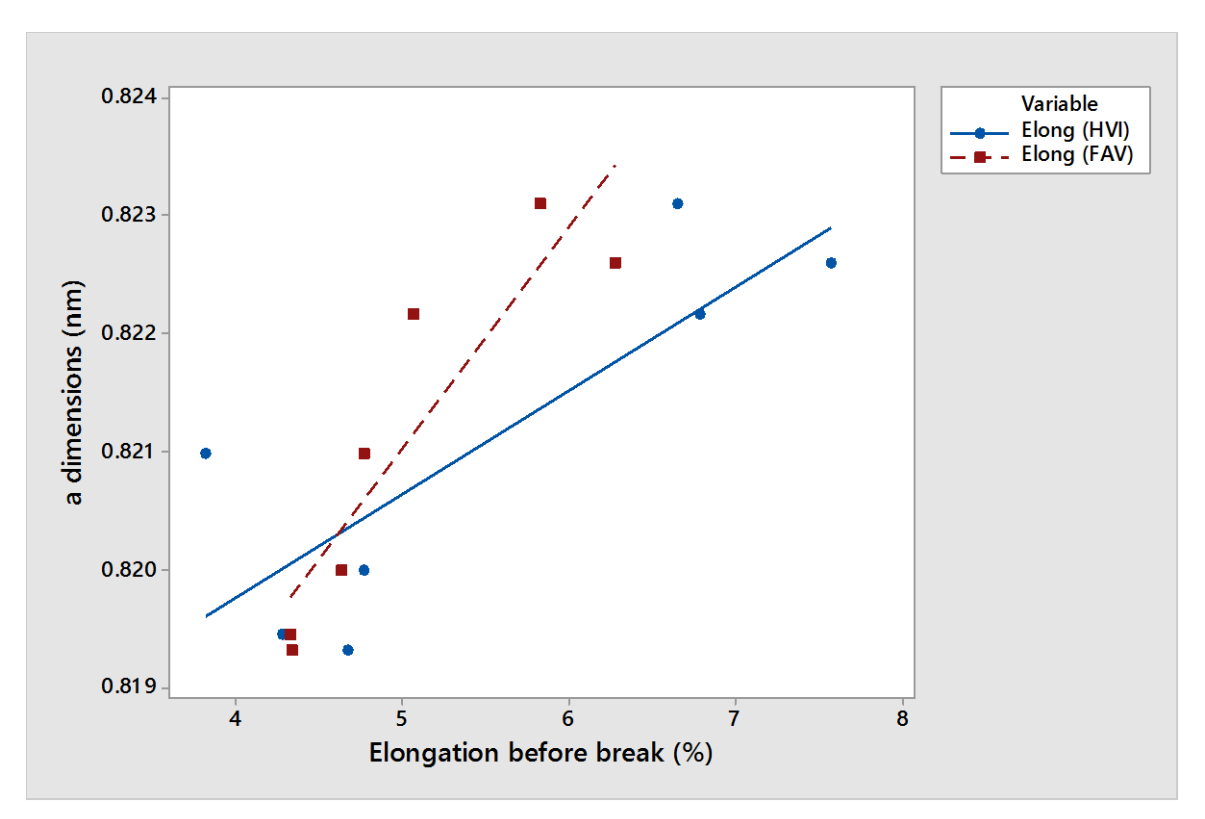


Figure 19 – Fibre elongation by HVI and Favimat with dimensions of the 'a' direction of the cellobiose unit in cellulose.

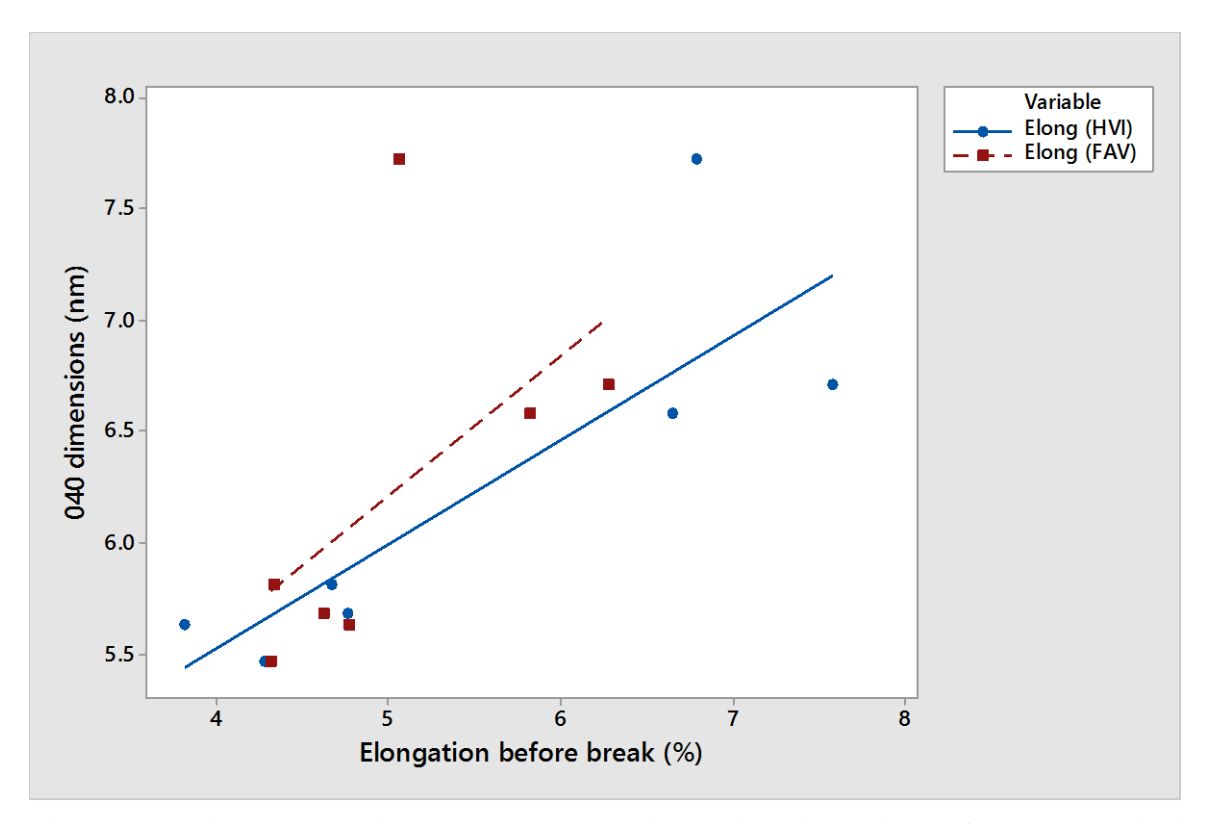


Figure 19 – Fibre elongation by HVI and Favimat with dimensions of the 040 lattice in cellulose.

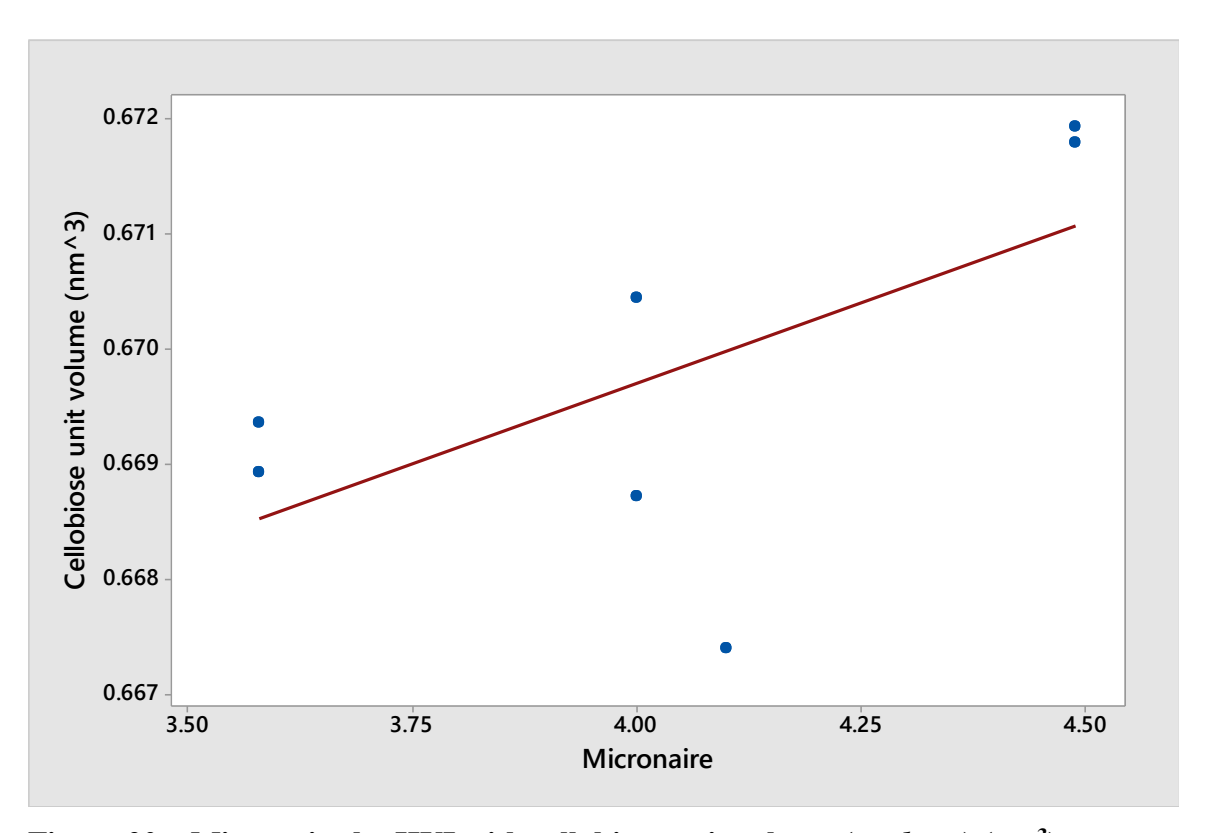


Figure 20 – Micronaire by HVI with cellobiose unit volume $(a \times b \times c)$ (nm^3)

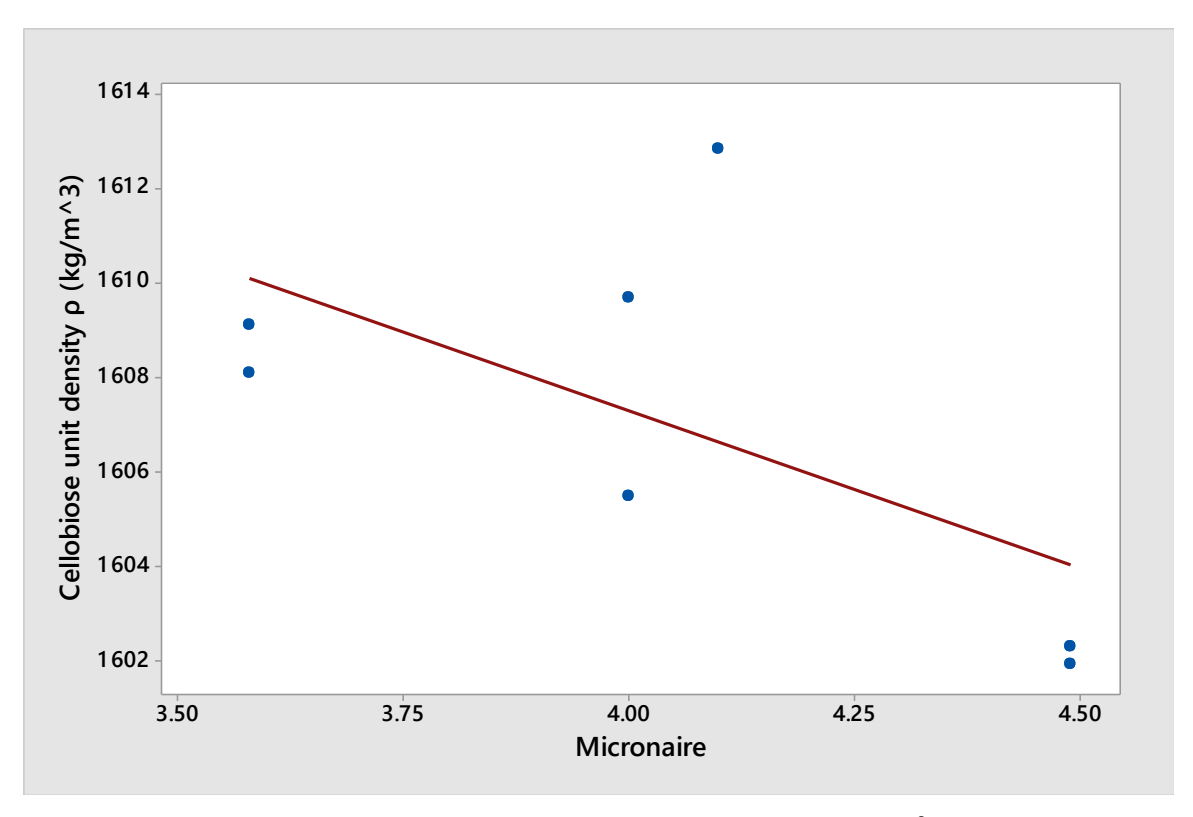


Figure 21 – Micronaire by HVI with cellobiose unit density (kg/m³)

FTIR-ATR Analysis

Figure 22 shows FTIR-ATR spectra for the seven samples across the wavelength numbers 3800-650 cm⁻¹. These show two ranges of high variance, between 3800-2600 cm⁻¹, particularly between 3200 and 3300 cm⁻¹, and 1800-650 cm⁻¹, particularly between 1550-1650 cm⁻¹. Figures 23-25 show plots of the eigenvalues, or proportion of variance, for each wavelength range. Across the whole spectra (3800-650 cm⁻¹), the first eigenvalue explained 50% of the recorded variation in the spectra. When the wavelength ranges were separated into the two observed ranges, i.e., 3800-2600 cm⁻¹ and 1800-650 cm⁻¹, the first eigenvalue of the 3800-2600 cm⁻¹ explained 80% of the variation, whilst explaining 50% of the 1800-650 cm⁻¹ range.

The range between 3200 and 3350 cm⁻¹ and specifically wavelengths at 3333 and 3284 cm⁻¹ corresponds with hydrogen-bonded O-H stretching regions in cotton. These bands shift depending on fibre development as shown by Cintrón and Hinchcliffe [17], who examined developing cotton fibres from 18 DPA through to 40 DPA. Figures 26 and 27 show XY plots of loading scores for each sample replicate for the 3800-2600 cm⁻¹ region. These show no strong grouping of samples, indicating the spectra were unable to properly delineate fibre samples on the basis of properties connected with the O-H stretching region.

Changes in the O–H band are attributed to signal strengthening of the corresponding hydrogen bonds, with stronger bonds shifting the corresponding O–H bands to lower energy. The attribution of these wavelengths to O-H stretching has mostly been applied as a result of testing wood samples, wherein higher frequencies at these wavelengths were noticed when specimens were subject to tension. For cotton, Cintrón and Hinchcliffe [17], were unclear if the observed changes measured in DPA samples arose arise from variations in surface O–H groups or a more intrinsic change in the cellulose composition of the fibres.

Figures 28 and 29 show XY plots of loading scores for sample replicates for the 1800-650 cm⁻¹ region. These also showed no clear distinction or groupings between samples. The wavelengths between 1500 and 1650 cm⁻¹, where the greatest amount of variation is observed, are attributable to the O-H bending region, which like the 3200 and 3300 cm⁻¹

region vary significantly during fibre development. The O-H bending region is associated with the capacity of cellulose to absorb water, which in turn is thought to reflect the dimensions of cellulose crystallites.

In contrast to the variation seen in the O-H stretching and bending bands, vibrational bands from C–O bonds at 1104, 1052 and 1028 cm⁻¹, which form the covalent skeleton of the glucose (cellobiose unit) chain (as per Figures 1, 2 and 3), showed little variation in intensity across the sample set.

Similar analyses of the FT-Raman spectra gave the same results, as did partial least squares analyses applied to the FTIR-ATR and FT-Raman spectra.

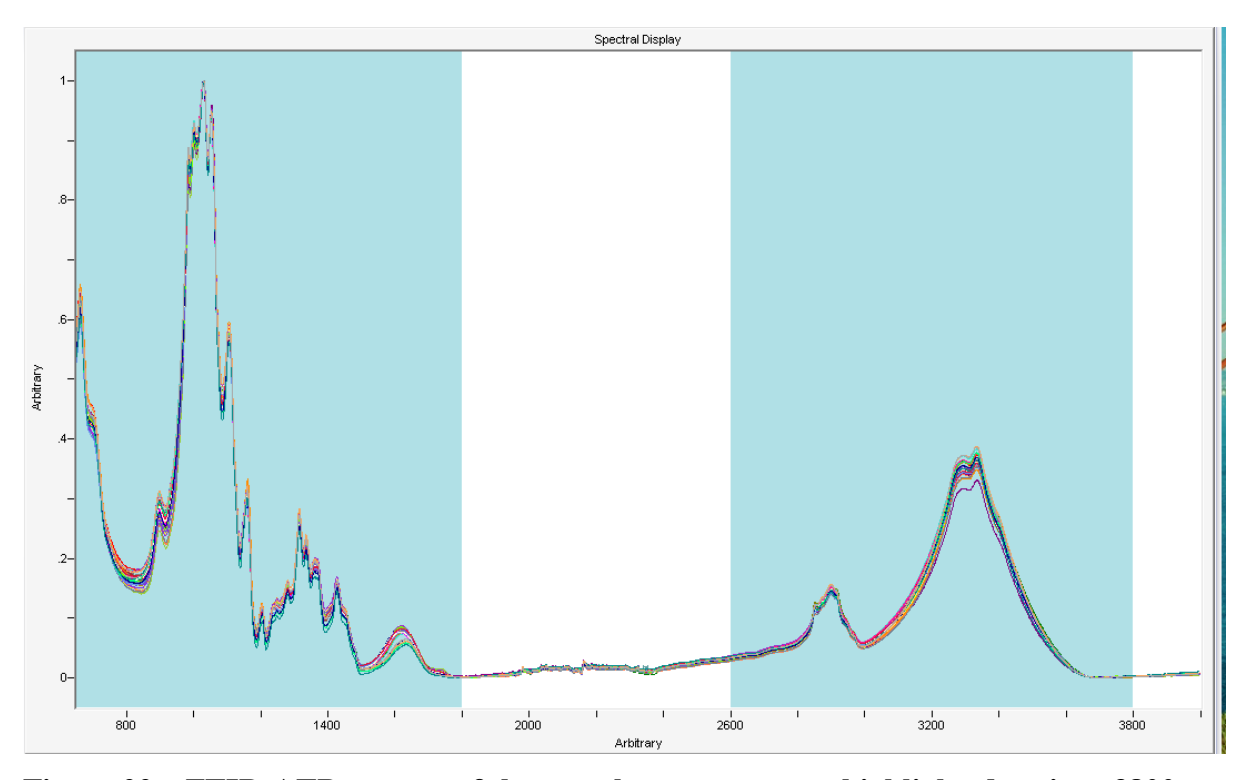


Figure 22 – FTIR-ATR spectra of the sample set across two highlighted regions 3800-2600cm⁻¹ and 1800-650cm⁻¹.

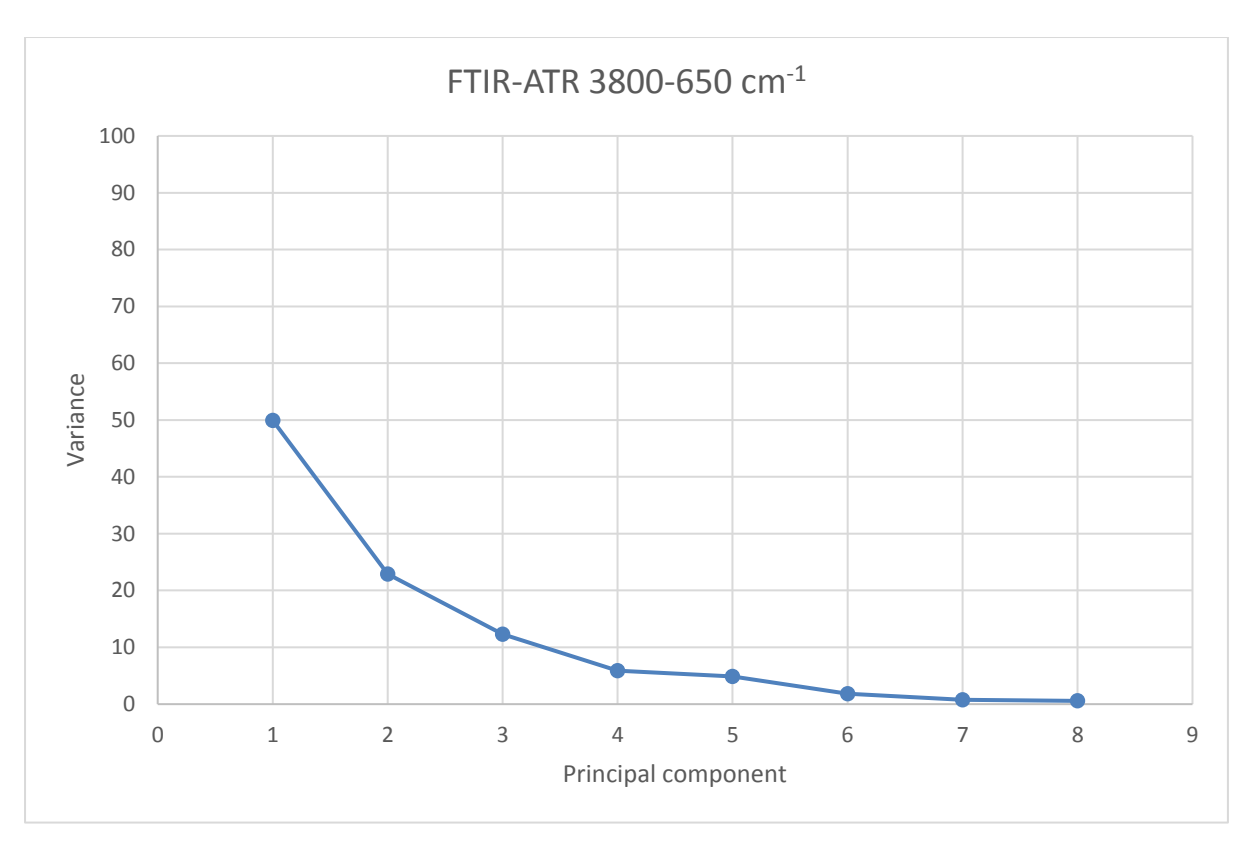


Figure 23 – Principal component variance for entire spectrum (3800-650 cm⁻¹)

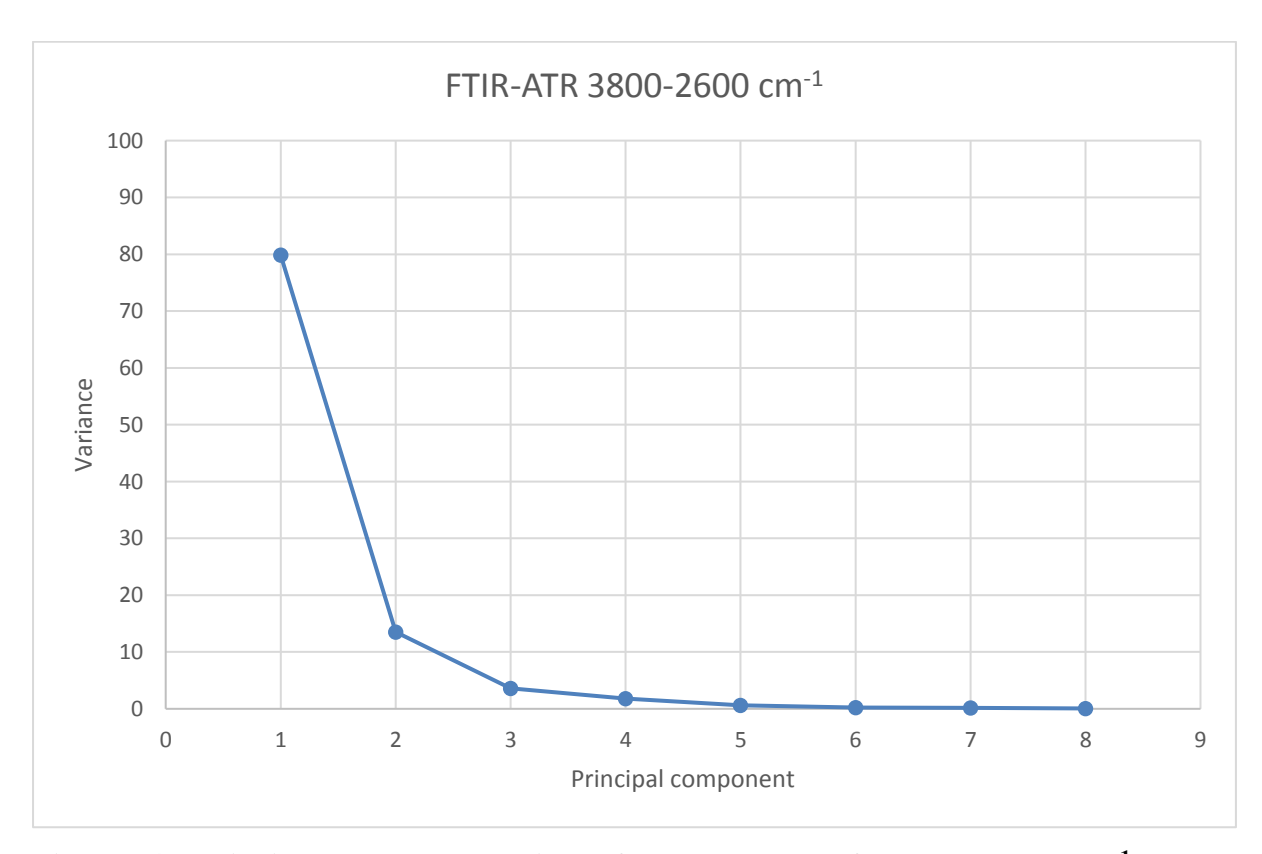


Figure 24 – Principal component variance for the spectrum from 3800-2600 cm⁻¹

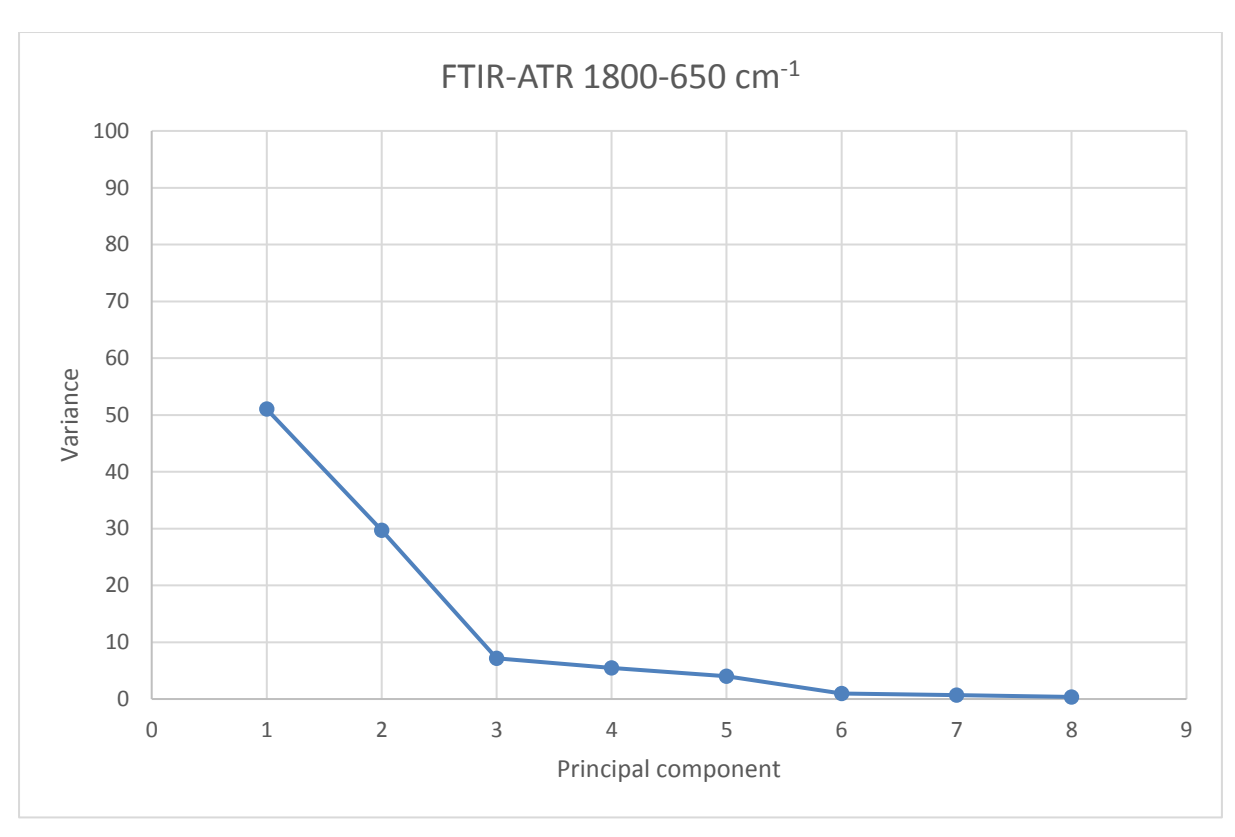


Figure 25 – Principal component variance for the spectrum from 1800-650 $\mbox{cm}^{\text{-}1}$

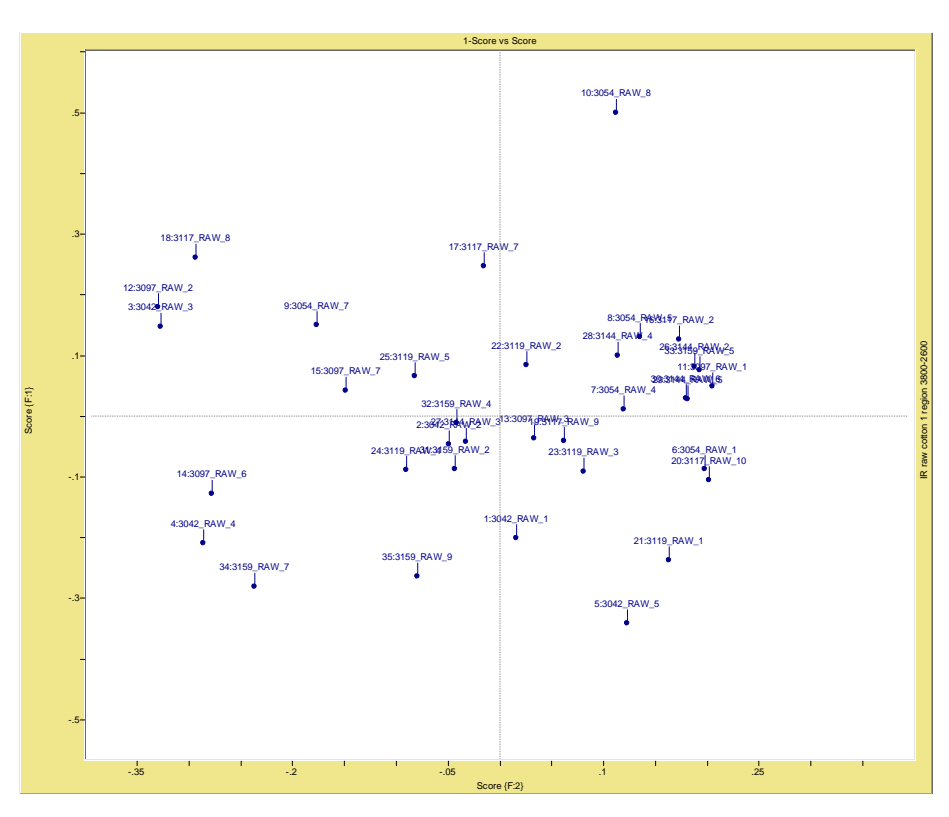


Figure 26 – PCA loading scores F1 and F2 for all samples (3800-2600 cm⁻¹ region)

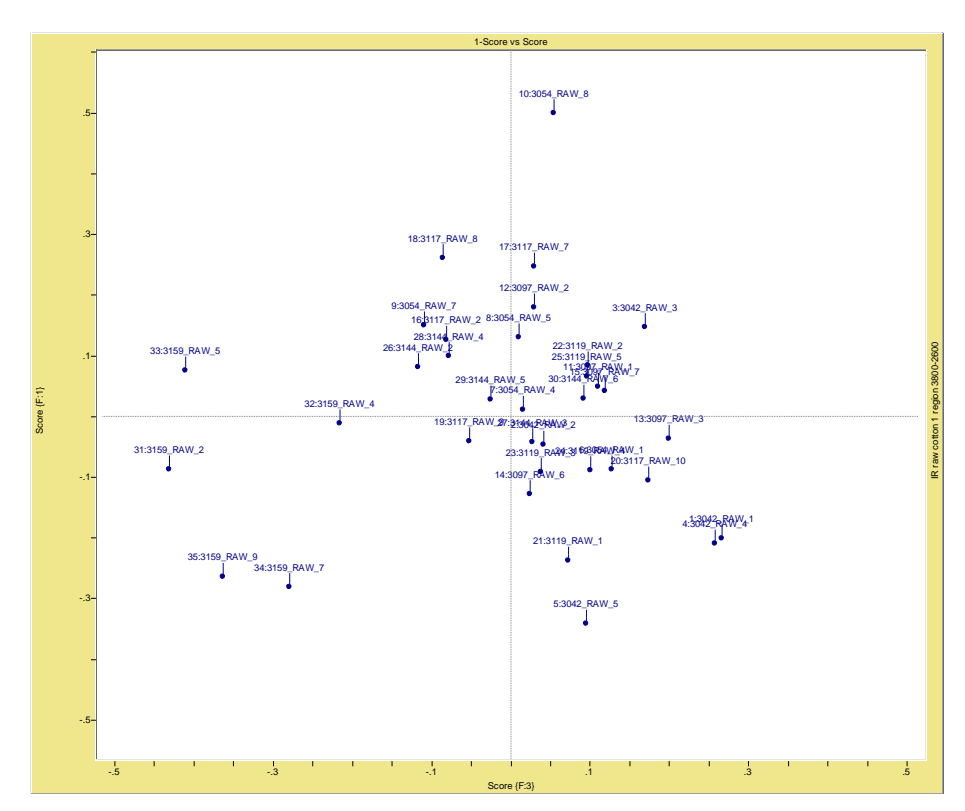


Figure 27 - PCA loading scores F2 and F3 for all samples $(3800 - 2600 \text{ cm}^{-1} \text{ region})$

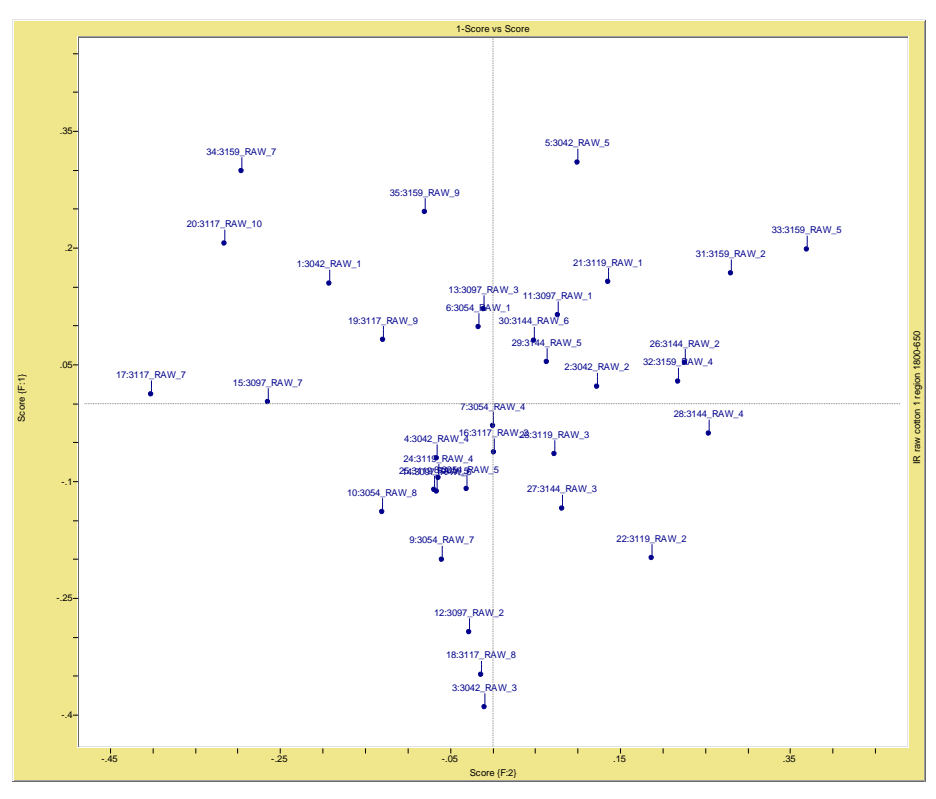


Figure 28 - PCA loading scores F1 and F2 for all samples (1800-650 cm $^{\text{-}1}$ region)

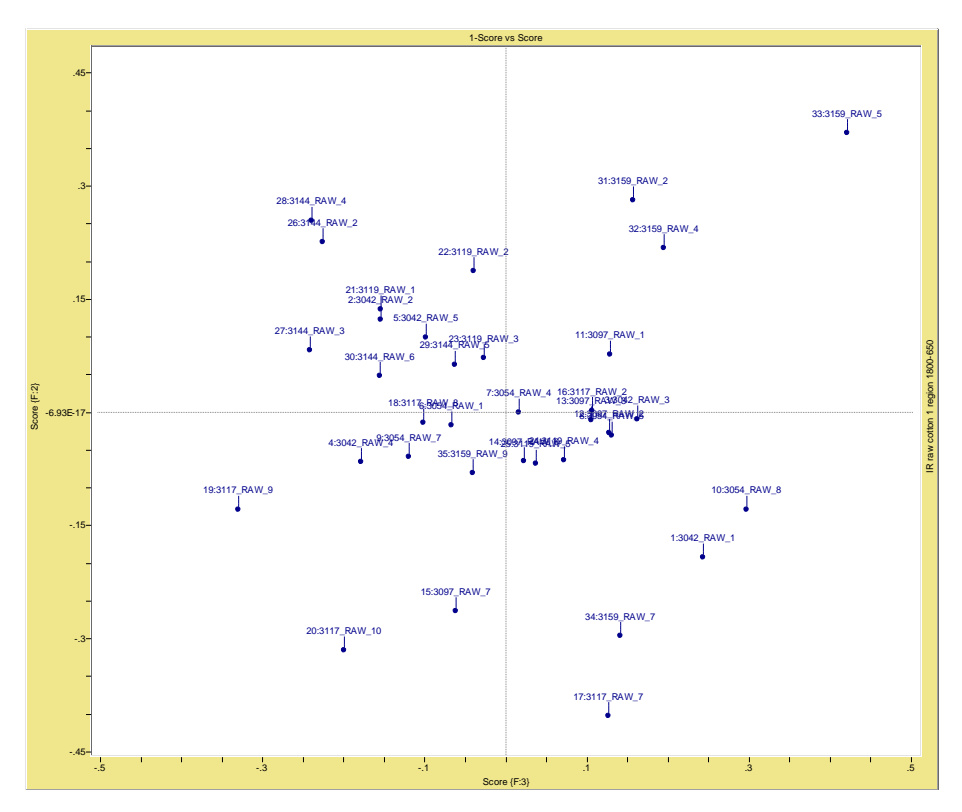


Figure 29 – PCA loading scores F2 and F3 for all samples (1800-650 cm⁻¹ region)

Confocal micro-Raman microscopy

The use of micro-Raman spectroscopy (beam) via an optical microscope was tested in this project. The particular application to single cotton fibres set longitudinally has not been reported previously and as such this investigation required determination of procedure (laser wavelength, slitting and power) and settings (fibre mount).

In one approach, Raman spectra were obtained using the microscope polarizing lenses to identify specific areas on the fibre to be analysed by the laser. Figure 30 shows a single mature fibre from Sample 3054 under the polarizing lenses of the confocal micro-Raman microscope. These allowed particular areas of the fibre to be highlighted and examined by the Raman laser. For example, features such as maturity (by colour difference) and the occurrence of reversals (in the cellulose helical structure) are apparent under crossed polarizing lenses.

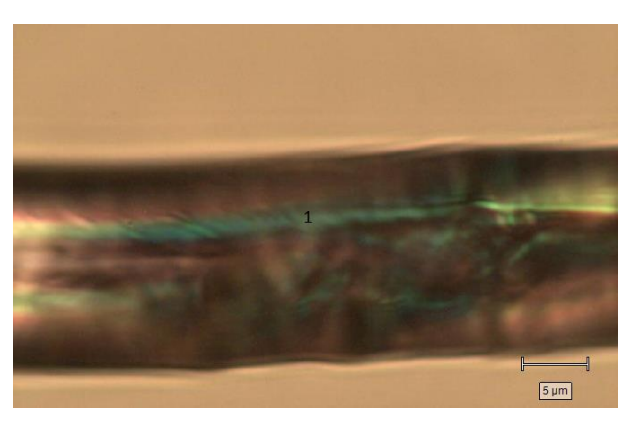


Figure 30 – Mature fibre from Sample 3054 mounted on a glass slide and held by double-sided tape at ends of the fibre (scale as shown). '1' highlights examined blue section.

The measured spectrum (Figure 31) was a result of a 10 s exposure and five co-added scans. The recorded spectra did not accord with cellulose spectra recorded by confocal Raman IR, e.g., as per Figure 32 from Cabrales *et al* [18] for fibre cross-sections. The measured spectra is missing peaks at 2800 cm⁻¹ and details at 1100-1600 cm⁻¹ and 400 cm⁻¹. The impediments for the collection of representative and consistent spectra included:

- Fitting a new laser to the instrument,
- A fault in the pin-hole aperture of the instrument, which did not functionally correctly and as such the laser could not be accurately pin-pointed on the sample and
- Interference from the glass microscope slide upon which the sample was mounted. It is important in this type of analysis to have the sample still and constant at a designated depth-of-field.

However, the application of this technique remains of interest, particularly its ability to survey of cellulose structure to prescribed depths along and through single fibres and, laser permitting, its resolution at a single micron scale.

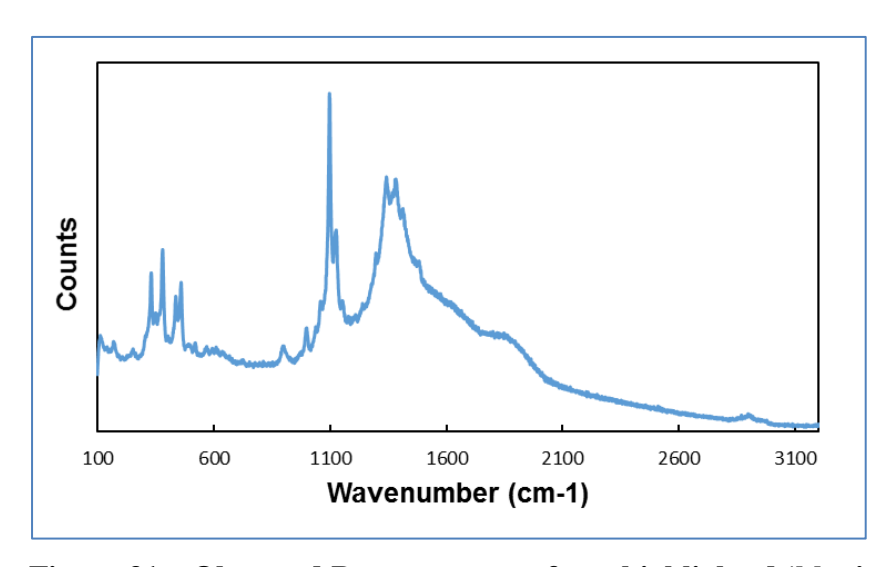


Figure 31 – Observed Raman spectra from highlighted 'blue' section of mature fibre from sample 3054.

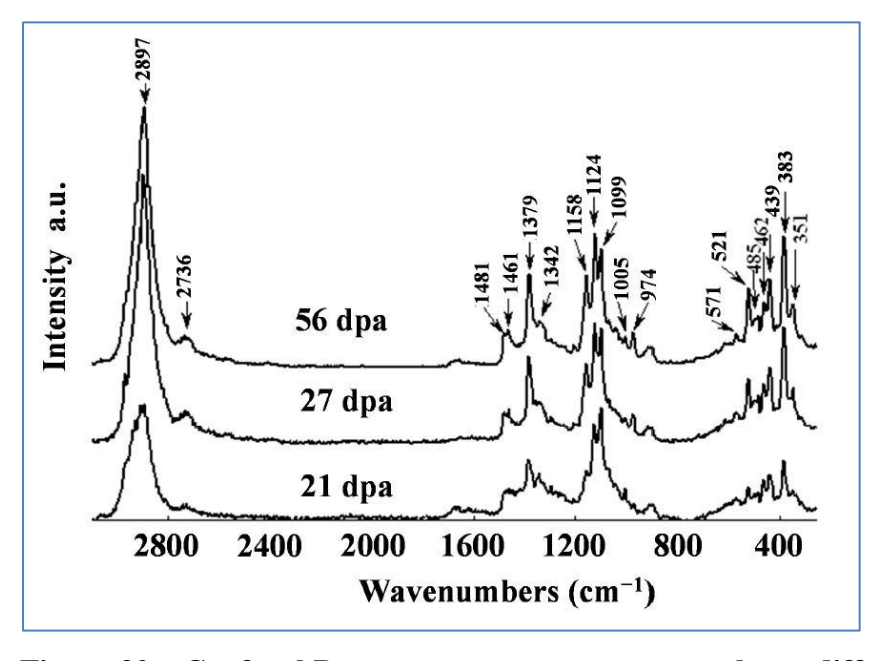


Figure 32 – Confocal Raman spectra on cotton samples at different DPA [18].

In another approach the same fibre (from Sample 3054) (Figure 33) was depth profiled using the instrument's confocal mode. In this mode the intensity of the entire spectrum reduces as the laser beam (of 514 nm) samples further into the fibre (Figure 34). A plot of the spectral intensity at 1096 cm $^{-1}$, attributed to C-O-C glycosidic link asymmetric stretching mode, is shown in Figure 34. It is thought the flat region between 6-8 μ m (Figure 35) into the fibre may represent the lumen.

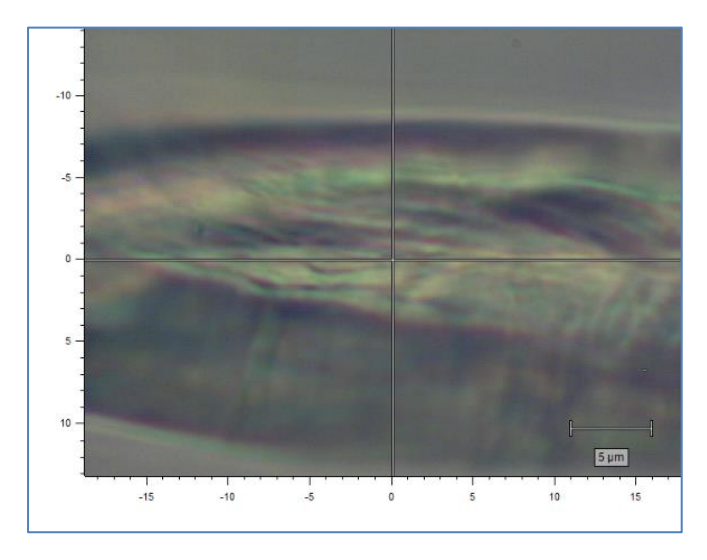


Figure 33 – Crosshairs show point of depth profile through Sample 3054.

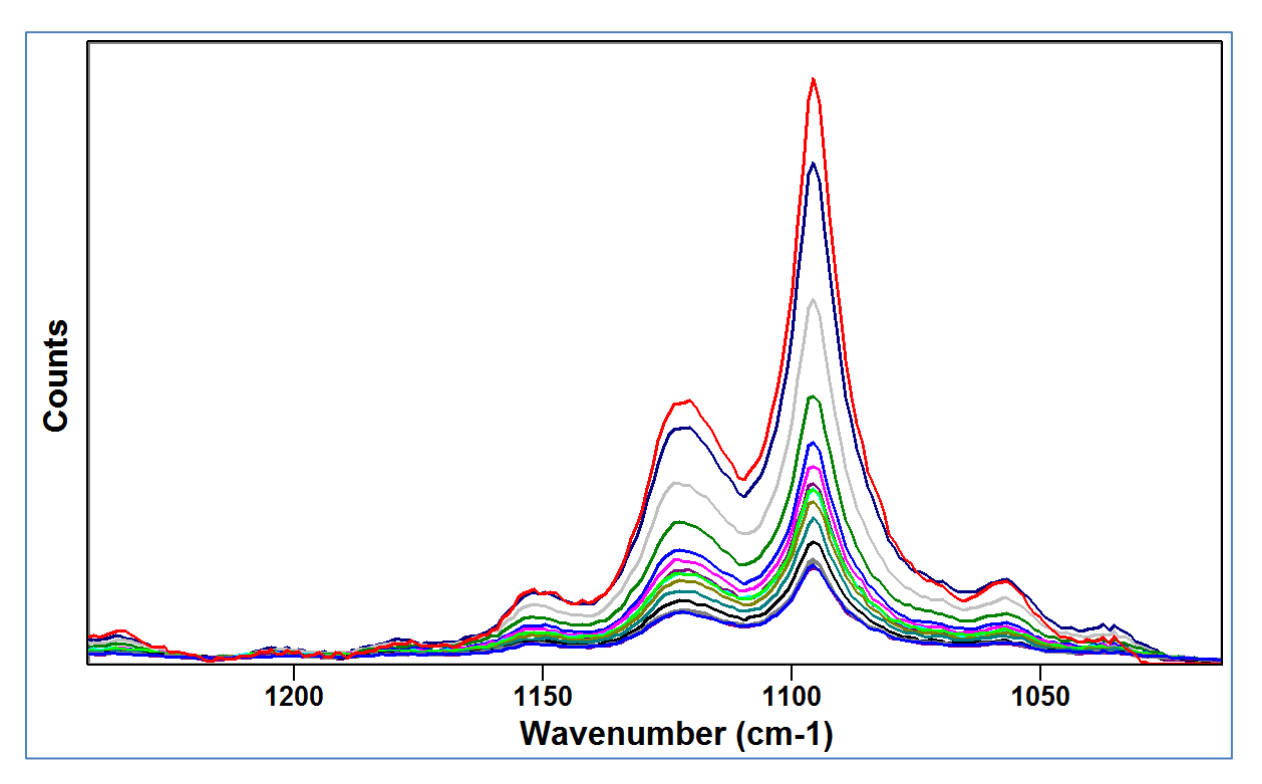


Figure 34 – Raman spectra through profile of Sample 3054 fibre at 1 µm increments.

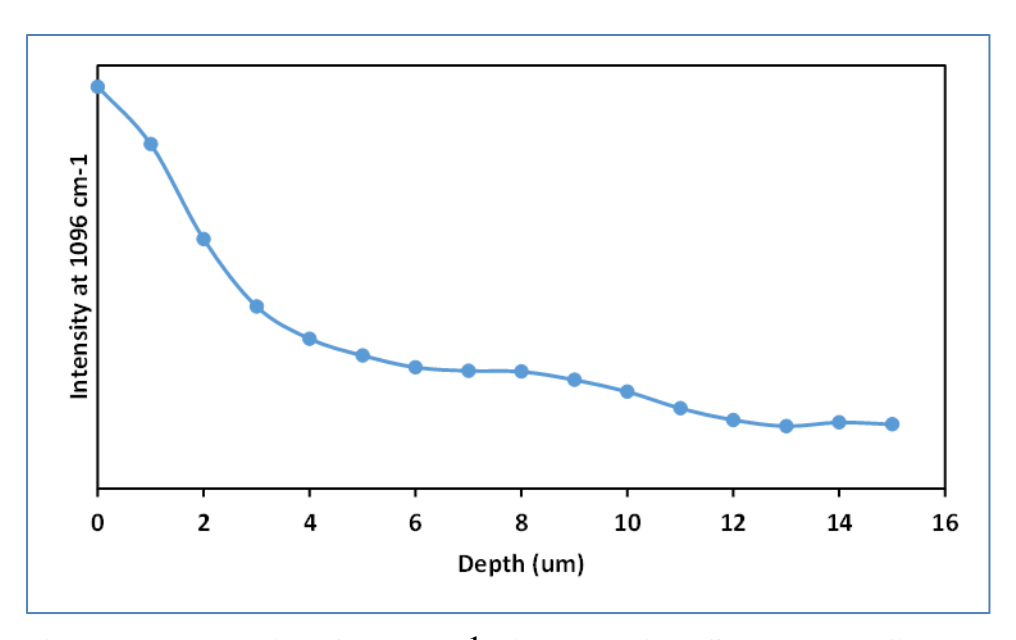


Figure 35 – Intensity of 1096 cm $^{\text{-}1}$ with depth into Sample 3054 fibre. Flattening between 6 and 8 μ m is suggested as being the position of the lumen.

References

- 1. Hu, X. P. and Hsieh, Y. L., (1996) Crystalline structure of developing cotton fibers. *J. Polym. Sci. Polym. Phys.*, 34: 1451–1459.
- 2. Hsieh Y. L, Hu, X. P. and Nguyen, A., (1997) Strength and crystalline structure of developing Acala cotton, *Textile Res. J.*, 67: 529–536.
- 3. Abidi, N. and Manike, M., (2017) X-ray diffraction and FTIR investigations of cellulose deposition during cotton fiber development, *Textile Res. J.*, DOI: 10.1177/0040517516688634
- 4. Liu, Y., Thibodeaux, D., Gamble, G. and Rodgers, J., (2014) Preliminary study of relating cotton fiber tenacity and elongation with crystallinity, *Textile Res. J.*, 84(17): 1829–1839.
- 5. Moore, Z., (2008) Application of X-ray diffraction methods and molecular mechanics simulations to structure determination and cotton fiber analysis, *University of New Orleans Theses and Dissertations*. Paper 888
- 6. Terinte, N., Ibbett, R. and Schuster, K. C., (2011) Overview on native cellulose and microcrystalline cellulose I structure studied by X-ray diffraction (WAXD): Comparison between measurement techniques, *Lenzinger Berichte*, 89: 118-131
- 7. Astbury, W. T., (1943), Textile Fibres under the X-rays, Imperial Chemical Industries Limited (Pub), 54 pages.
- 8. Meyer, K. H. and Misch, L., (1937) Helv. Chem. Acta, 20: 232.
- 9. Frey-Wyssling, V. A. and Mühlethaler, K. (1963), Die elementarfibrillen der cellulose. *Makromol. Chem.*, 62: 25–30. doi:10.1002/macp.1963.020620103
- 10. Wright, N., Long, R., Evans, R. and Gordon, S., (2011) Characterising strength related structures in cotton fibres by XRD on the Australian Synchrotron and on SilviScan, Australian X-ray Analytical Association Conference, Sydney NSW, Feb 2011.
- 11. Liu, Y. (2013), Recent progress in Fourier Transform infrared (FTIR) spectroscopy study of compositional, structural and physical attributes of developmental cotton fiber, *Materials* 6, 299-313; doi:10.3390/ma6010299
- 12. ASTM D1442 06, (2012) Standard Test Method for Maturity of Cotton Fibers (Sodium Hydroxide Swelling and Polarized Light Procedures).
- 13. Patterson, A., (1939) The Scherrer formula for X-Ray particle size determination, *Phys. Rev.* 56(10): 978–982.
- 14. Foreman, D. W. and Jakes, K. A., (1993) X-Ray Diffractometric measurement of microcrystallite size, unit cell dimensions and crystallinity: Application to cellulosic marine textiles, *Textile Res. J.*, 63(8): 455-464.
- 15. Boylston, E. K., Thibodeaux, D. P. and Evans, J. P., (1993) Applying Microscopy to the Development of a Reference Method for Cotton Fiber Maturity, *Textile Res. J.*, 63(2): 80-87
- 16. Hequet, E., Wyatt, B., Abidi, N and Thibodeaux, D., (2006) Creation of a set of reference material for cotton fiber maturity, *Textile Res. J.*, 76(7): 576-586.
- 17. Cintrón, M. S. and Hinchcliffe, D. J., (2015) FT-IR examination of the development of secondary cell wall in cotton fibers, *Fibers* 3: 30-40
- 18. Cabrales, L., Abidi, N. and Manciu, F., (2014) Characterisation of developing cotton fibers by confocal Raman microscopy, *Fibers*, 2: 285-294.

- 5. Please describe any:
 - a) technical advances achieved (eg commercially significant developments, patents applied for or granted licenses, etc.);
 - b) other information developed from research (eg discoveries in methodology, equipment design, etc.); and
 - c) required changes to the Intellectual Property register.

This project has identified new analytical techniques to survey the structural properties of single cotton fibres. Investigations using these techniques revealed that the unit cell 'a' and 002 lattice dimensions correlate closely with fibre tenacity and elongation as measured by Favimat, and that the 040 and 101 lattice dimensions correlate closely with fibre maturity as measured by Cottonscope.

Conclusion

6. Provide an assessment of the likely impact of the results and conclusions of the research project for the cotton industry. What are the take home messages?

Further survey work is required to confirm these relationships. Understanding the extent and variation of these structural properties in new cultivars, and in relation to the biochemistry and genetics driving maturation of the cotton fibre cell wall, will be important in developing better quality cotton fibre, particularly in terms of tenacity (strength) and elongation.

Extension Opportunities

- 7. Detail a plan for the activities or other steps that may be taken:
 - (a) to further develop or to exploit the project technology.
 - (b) for the future presentation and dissemination of the project outcomes.
 - (c) for future research.

The results from this investigation will be published in a reputable journal, e.g., Cellulose.

The project team will pursue funding opportunities so they can further investigate (i) the techniques developed in this project and (ii) the variation and extent of structural properties in new Australian cultivars.

9. A. List the publications arising from the research project and/or a publication plan. (NB: Where possible, please provide a copy of any publication/s)

NA

B. Have you developed any online resources and what is the website address?

NA

Part 4 – Final Report Executive Summary

Provide a one page Summary of your research that is not commercial in confidence, and that can be published on the World Wide Web. Explain the main outcomes of the research and provide contact details for more information. It is important that the Executive Summary highlights concisely the key outputs from the project and, when they are adopted, what this will mean to the cotton industry.

The objective of this project was to further investigate the relationship between cotton cellulose's crystalline structure and the fibre's tensile properties, as affected by chemical, genetic and/or environmental effects. In the end, because of time constraints, the variation in tensile properties as a result of these effects was not explored. Instead a select, well described group of fibre samples, controlled for micronaire, but with a wide range of tensile properties, in particular elongation, was selected for examination.

Whilst the application of IR spectroscopy and X-ray diffraction (XRD) to analyse the structure of cellulose is not new, this study utilised techniques not previously applied in the examination of cotton's crystallite structure. These included the application of the Australian Synchrotron SAXS/WAX beamline to aligned arrays of single mature and immature fibres and the use of a confocal micro-Raman microscope with a polarizing lens to identify and measure different areas within single fibres. More routine measurements of fibre bundles using Fourier Transform Infrared Attenuated Transmission Reflectance (FTIR-ATR) and Raman spectroscopy were also made.

This project has identified new analytical techniques to survey the structural properties of single cotton fibres. Investigations using these techniques revealed that the cellulose unit cell 'a' and 002 lattice dimensions correlate closely with fibre tenacity and elongation as measured by Favimat, and that the 040 and 101 lattice dimensions correlate closely with fibre maturity as measured by Cottonscope. The clarity of these relationships was clear and surprising given that work by other researchers has previously not been able to separate mature, commercial samples on the basis of these structural properties.

Further survey work is required to confirm these relationships. Understanding the extent and variation of these structural properties in new cultivars and in relation to the biochemistry and genetics driving maturation of the cotton fibre cell wall will be important in developing better quality cotton fibre, particularly in terms of tenacity (strength) and elongation.

APPENDIX 1

Australian Synchrotron SAXS/WAX beamline technical specifications

Source	In-vacuum undulator, 22 mm period, 3 m length, K _{max} 1.56
Energy range	5 - 21 KeV. Optimised for 8.15 KeV and 11.00 KeV.
Energy resolution	10 ⁻⁴ from cryo-cooled Si(111) double crystal monochromator.
	Horizontal and vertical focussing mirrors for monochromatic beam with variable focus for different camera lengths.
Mirrors	3 mirror stripes (Si, Rh, Pt) allow full coverage of energy range rejecting higher energy harmonics. Mirrors may be removed for speciality experiments.
	1 1
Maximum flux at sample	2×10^{13} photons per second.
waximum nux at sample	10 KeV, Si-111 DCM, 200 mA ring current.
Beam size at sample	250 μm horizontal × 150 μm vertical (FWHM)
(sample position focus)	Smaller beam size achievable by slitting down.
Beam divergence at	140-260 μrad horizontal; 30 - 60 μrad vertical depending
sample position	on focal position.
	SAXS - 0.0015 - 1.1 Å-1 (using multiple camera lengths)
q-range	WAXS - 0.5 - 10 Å ⁻¹ (using multiple detector angles)
Instrument background	Minimum $< 0.02 \text{ cm}^{-1} @ 0.01 \text{ Å}^{-1}$

APPRENDIX 2

AS PROPOSAL 8414

APPENDIX 3

AS PROPOSAL 10068